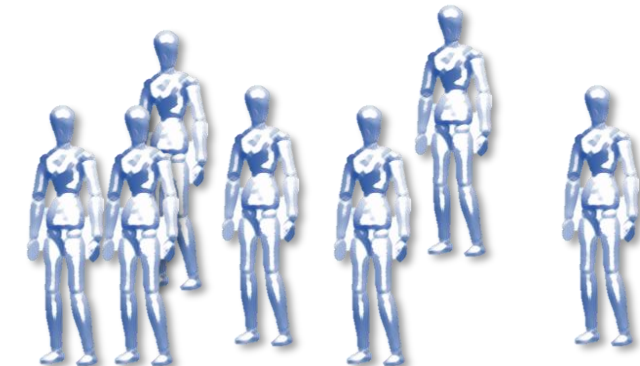
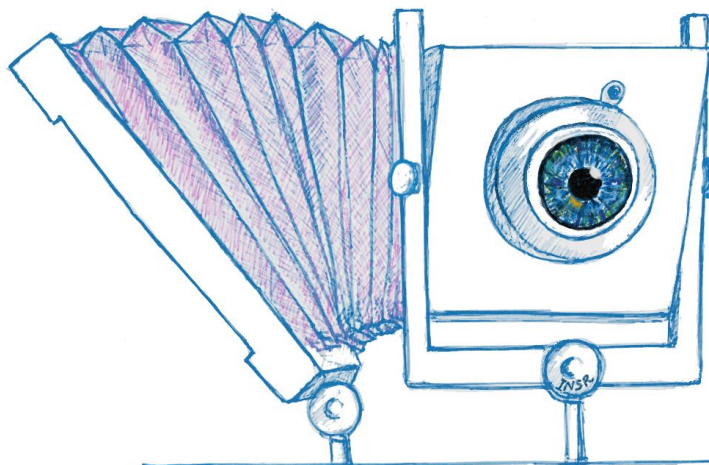


Scheimpflug with Computational Imaging to Extend the Depth of Field of Iris Recognition Systems

Indranil Sinharoy

Committee:

- Dr. Marc P. Christensen
- Dr. Delores M. Etter
- Dr. Dinesh Rajan
- Dr. Panos Papamichalis
- Dr. Yunkai Zhou



Unique

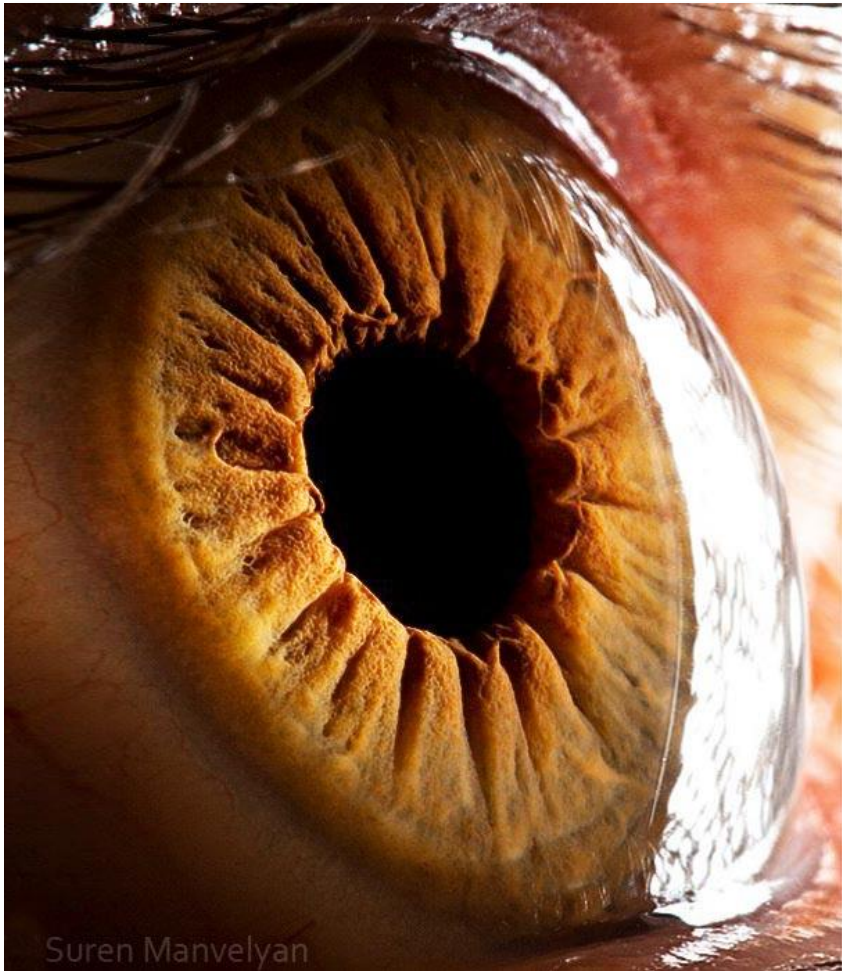
1



2

[Photographs by Jon Miles, milesresearch.com]

Several desirable properties of the iris pattern make it an ideal biometric



- Unique
- Stable over time
- Protected by the cornea from tampering
- Easily accessible

Iris recognition technology has great potential for providing robust surveillance



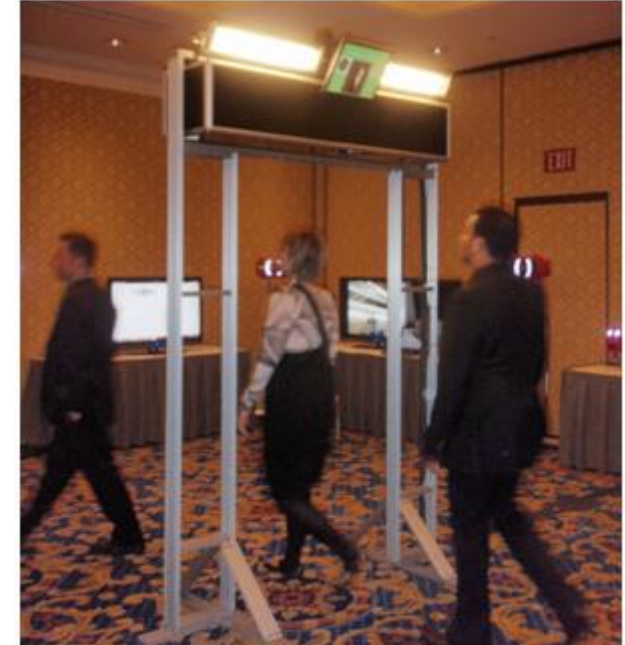
Hitherto, iris recognition has been restricted to close-range & well-controlled spaces



[CANPASS Air Iris Recognition System, biometricwatch.com, 2007]

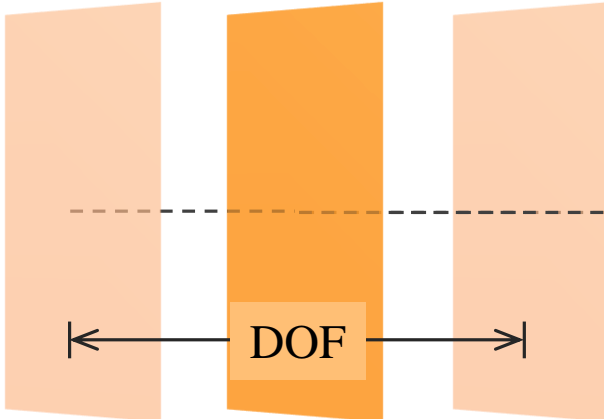


[AOptix Technologies, Inc, asis.confex.com/asis/ansem2010/webprogram/Session24387.html]



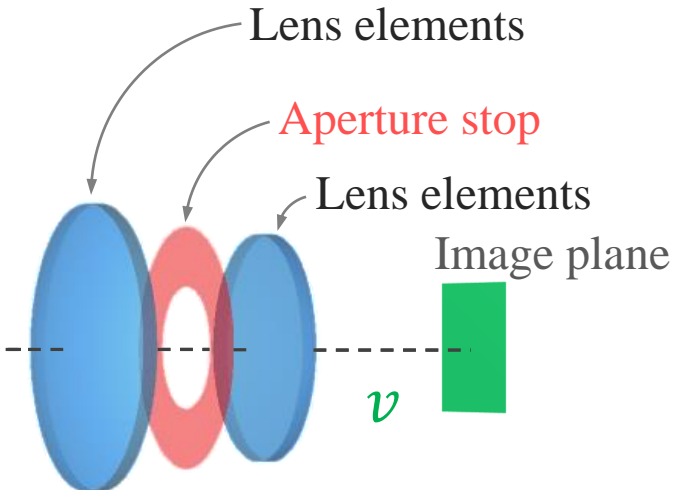
[Hoyos Corp. & Stanley CSS demo., Photo by Geoff Kohl, Security InfoWatch, 2011]

The depth of field (DOF) is the limited range of distances in the scene within which subjects appear sharp in the image



Plane of
sharp focus
(PoSF)

$-u$

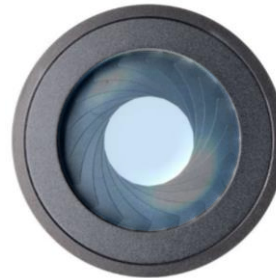


Gaussian formula: $\frac{1}{-u} + \frac{1}{v} = \frac{1}{f}$

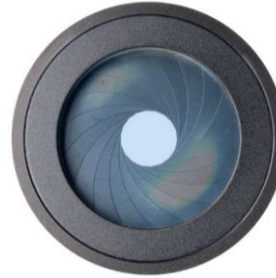
Shallow DOF



F/5.6



F/8



F/11

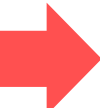


F/16

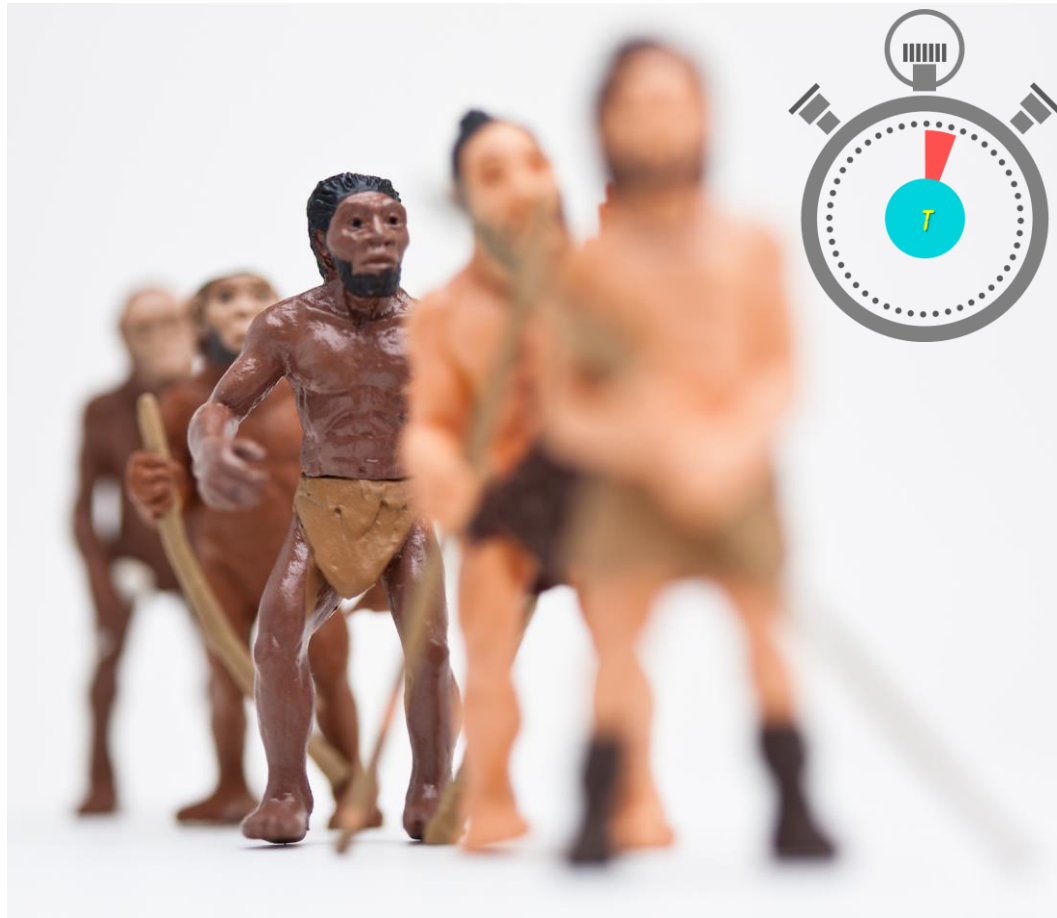


F/22

Large DOF



In traditional cameras the DOF is usually controlled by the aperture

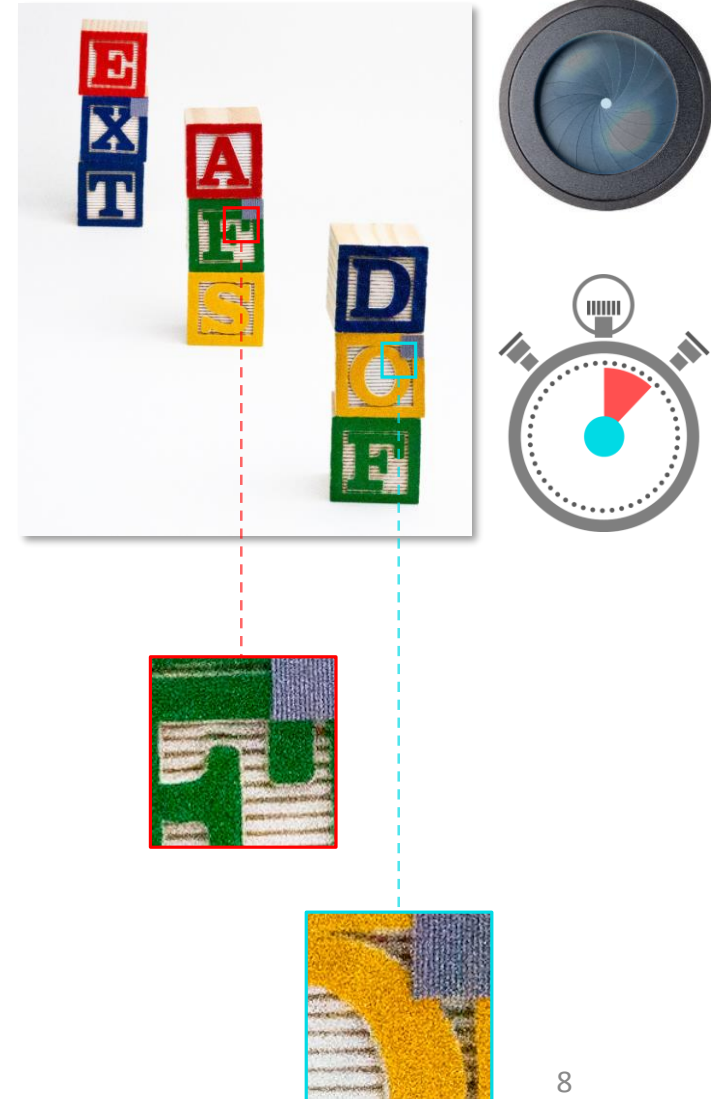
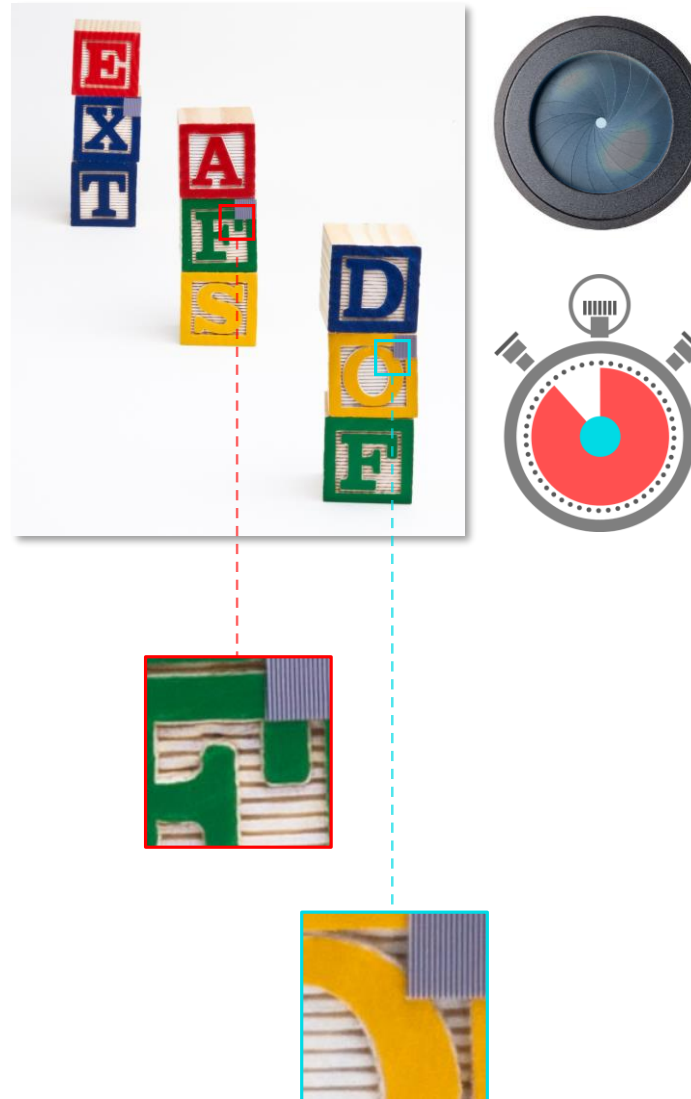
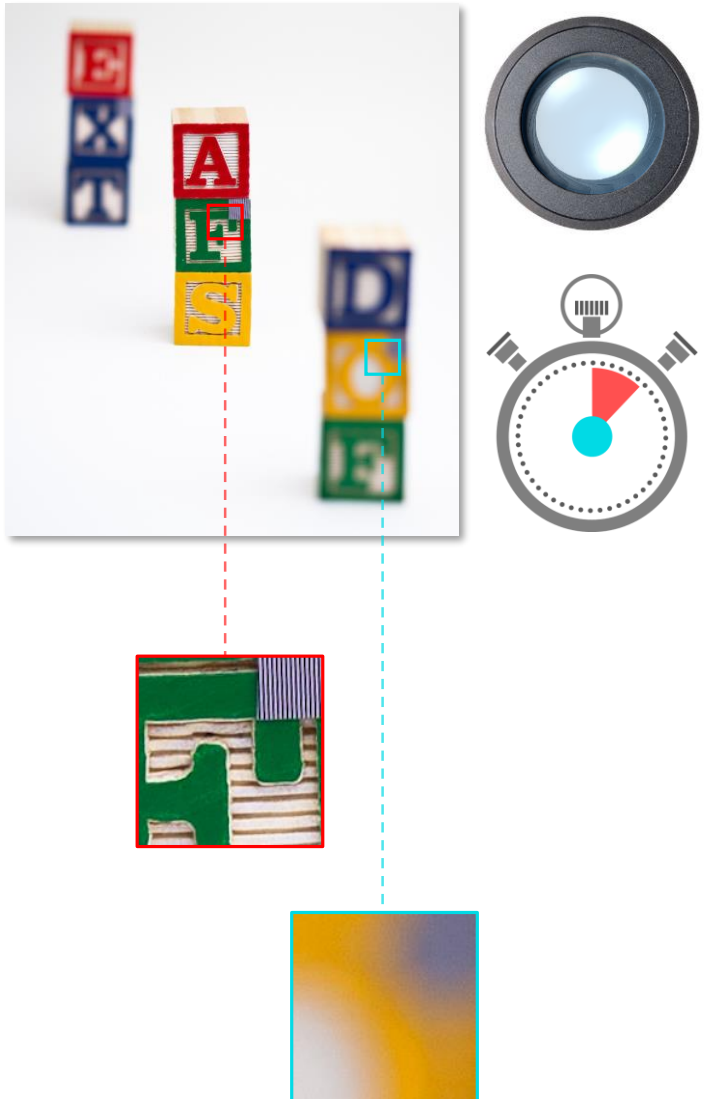


Shallow DOF, aperture: F/2.8

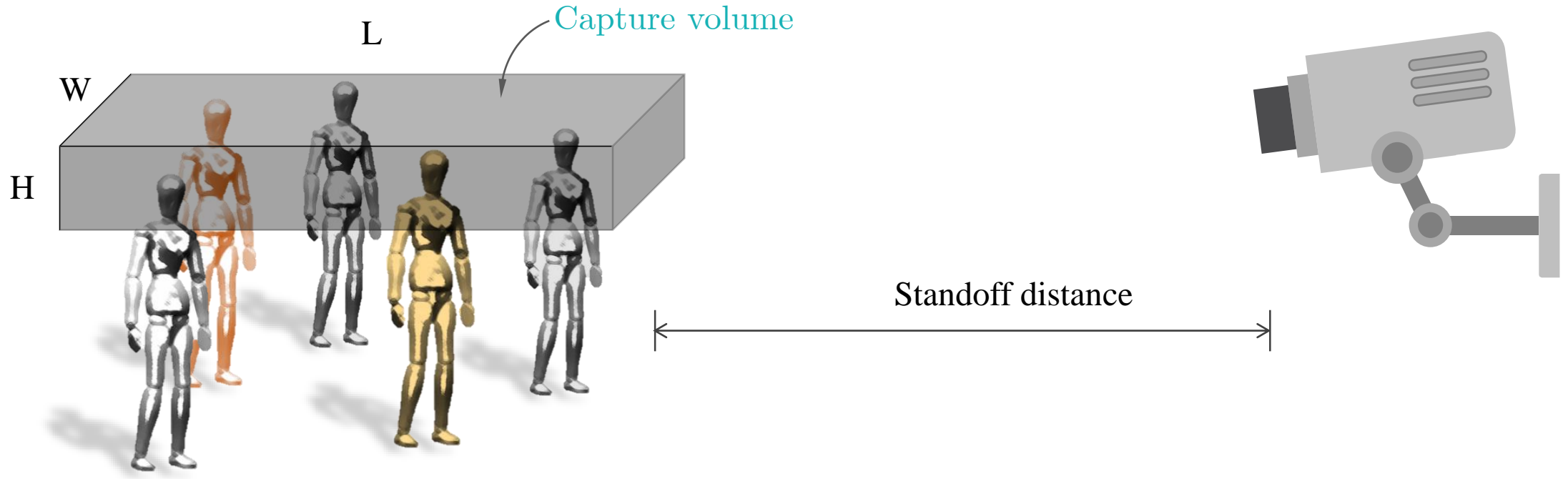


Large DOF, aperture: F/32

It is impossible to get high resolution, large DOF & high SNR simultaneously in traditional imaging



Increasing the DOF of the iris camera is an effective way of increasing the capture volume



The goal in this work is to extend the capture volume of iris recognition systems

What is an ideal solution?

- Extend the capture volume significantly (comparable or better than existing solutions)
- Scalable
- Low computational complexity for real time operation
- Low cost

The original contributions of this thesis

1. New pair of general imaging models
 - Lens and the sensor planes can freely rotate about independent pivots
 - Pupil parameters enable accurate and efficient estimation of geometric image properties
2. A new computational imaging approach for extending the depth of field of imaging systems
3. Conference paper, Imaging and Applied Optics Congress 2016
 - Won Best Multimedia Award ()
4. Journal paper submitted to OSA Applied Optics (stage: in peer review)
5. Software library for automating and externally controlling optical design and simulation tasks in Zemax
6. Invention disclosure (stage: patent being written by a lawyer)

Background

The new models

New comp.
imaging method:
Angular Focus
Stacking (AFS)

Zemax
simulation

Experimental
results



Existing solutions for extending the capture volume are either costly or plagued by noise

Two main class of solutions:

1. Multiple field of view stitching over space and/or time are costly
2. Wavefront coding—e.g. Cubic Phase Mask—exhibit low SNR at high spatial frequencies

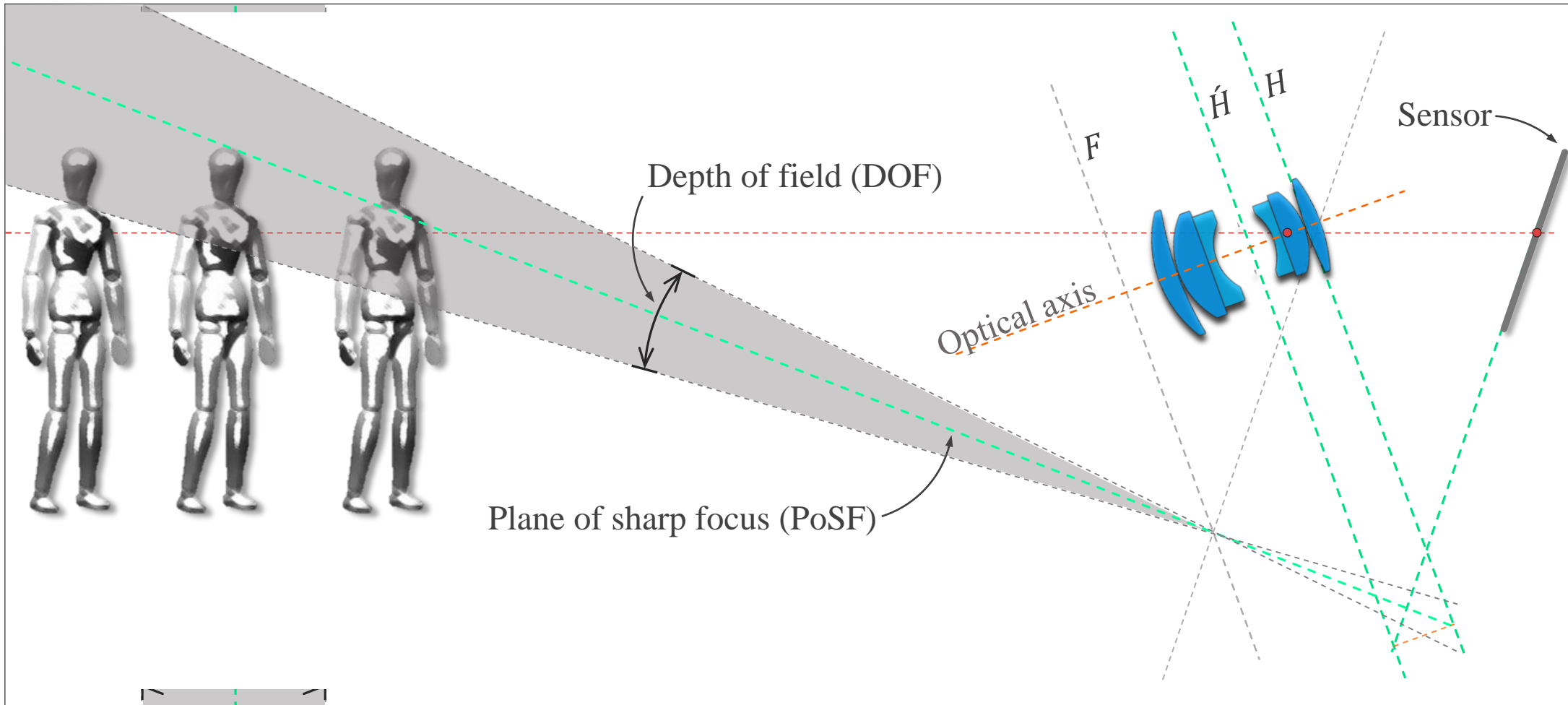
The lens & sensor in a Scheimpflug camera can rotate about independent pivots



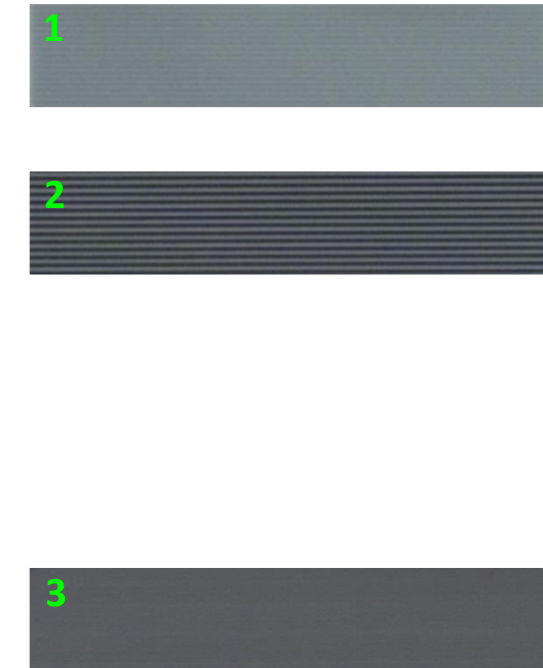
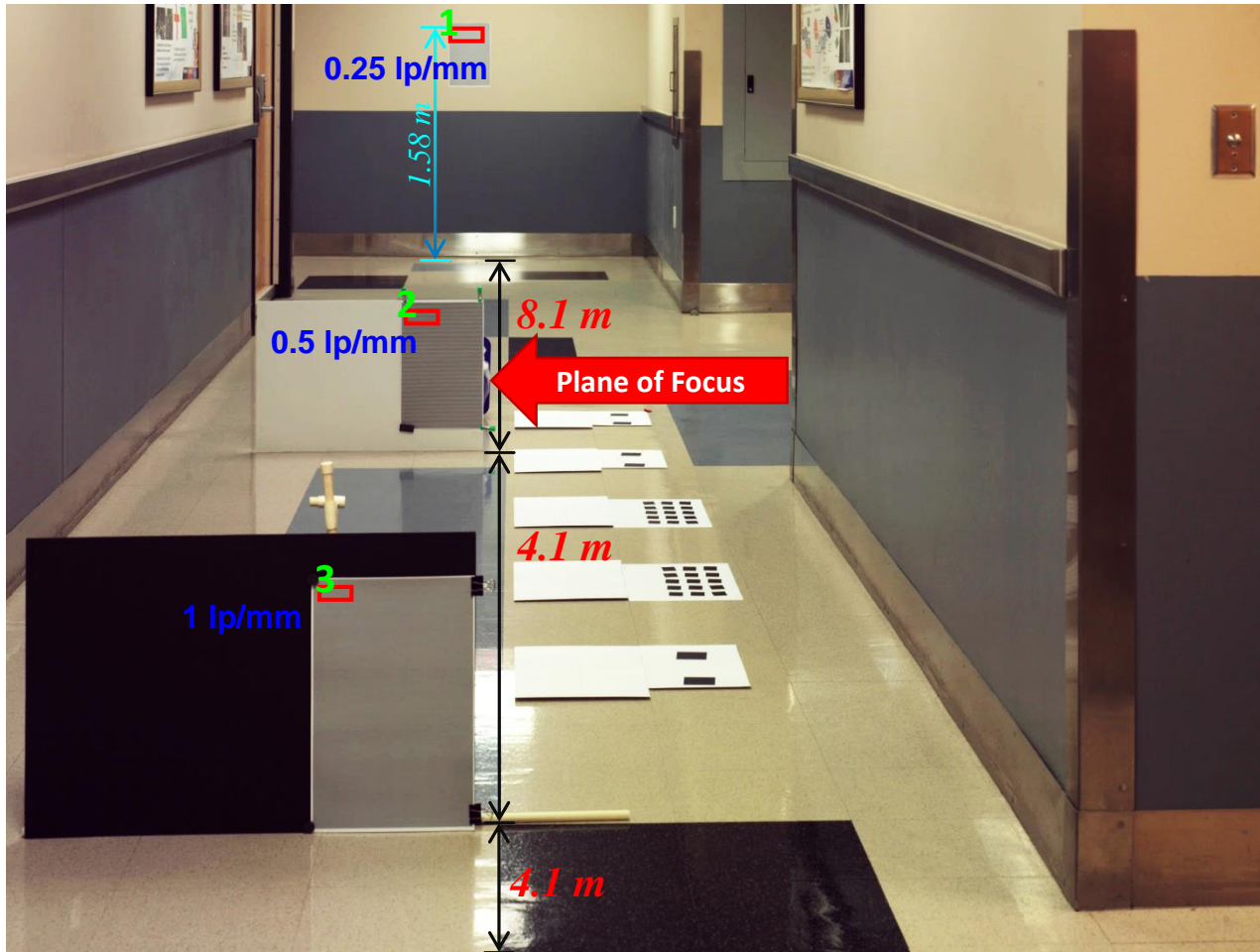
The lens & sensor in a Scheimpflug camera can rotate about independent pivots



Scheimpflug principle: Rotating the lens or the sensor also rotates the plane of sharp focus

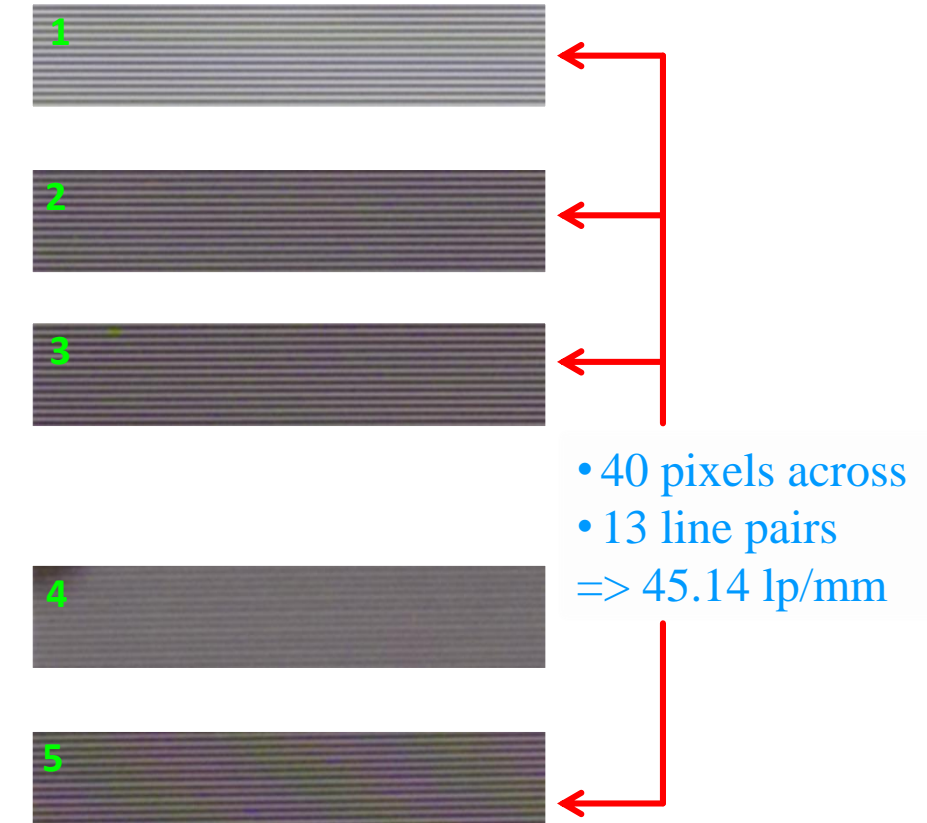
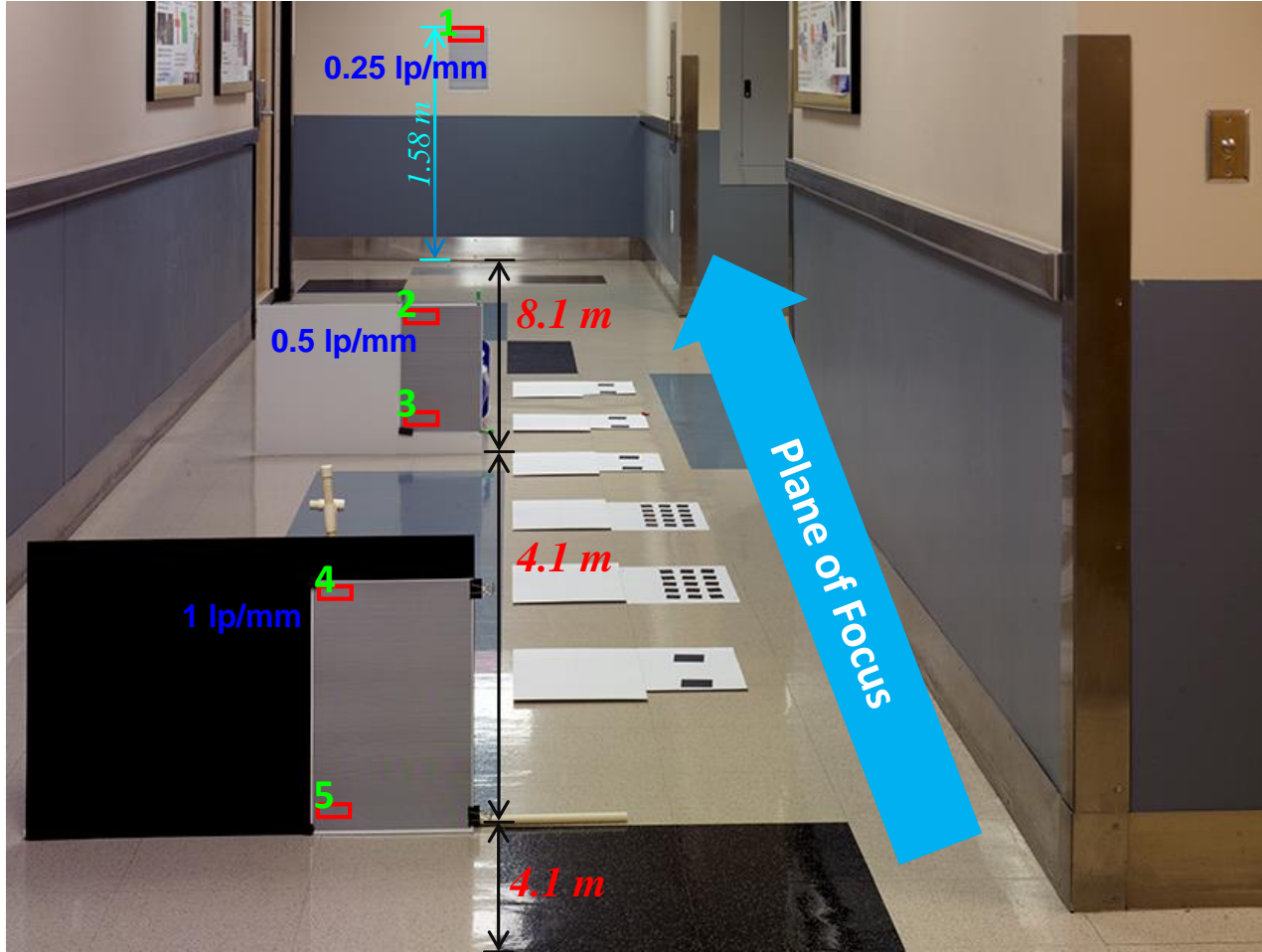


Initial experiments suggested the optics in the camera was great

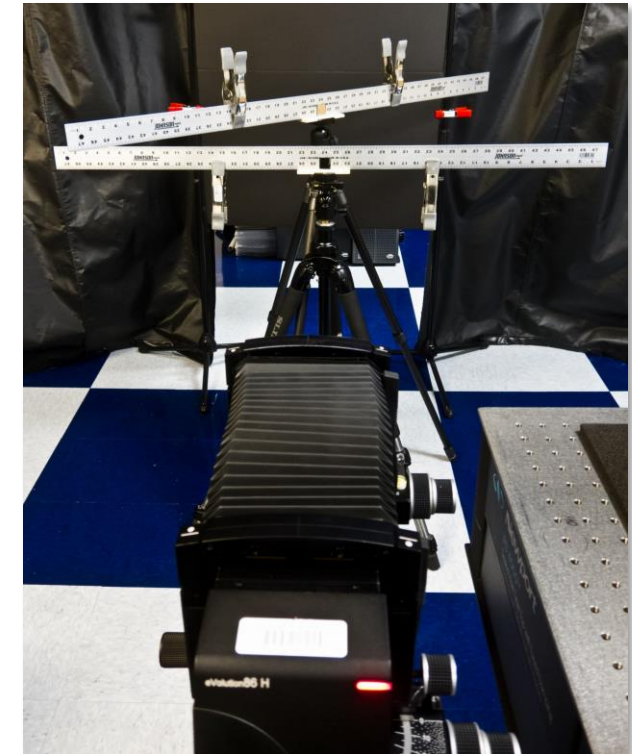
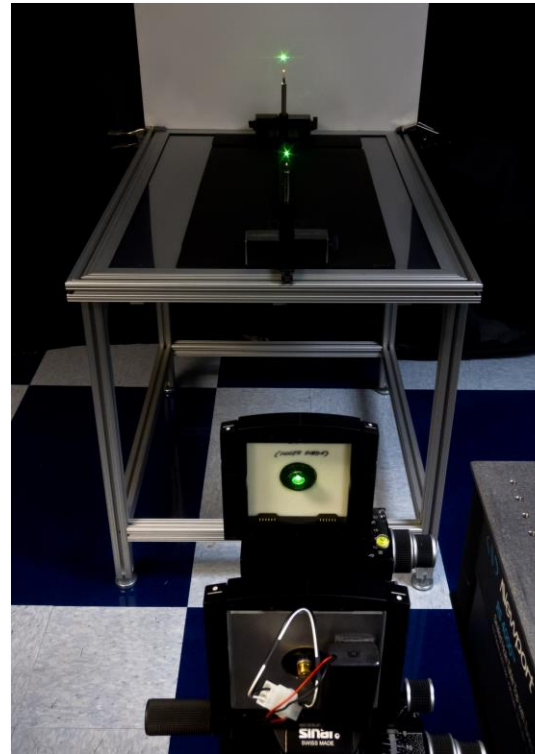
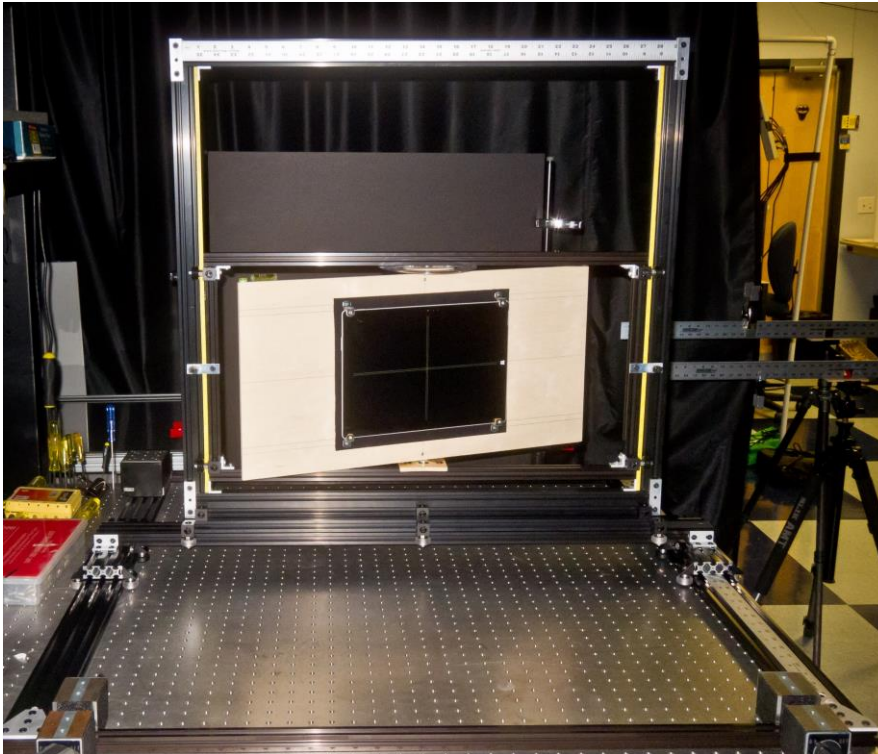


- 40 pixels across
 - 13 line pairs
- => 45.14 lp/mm

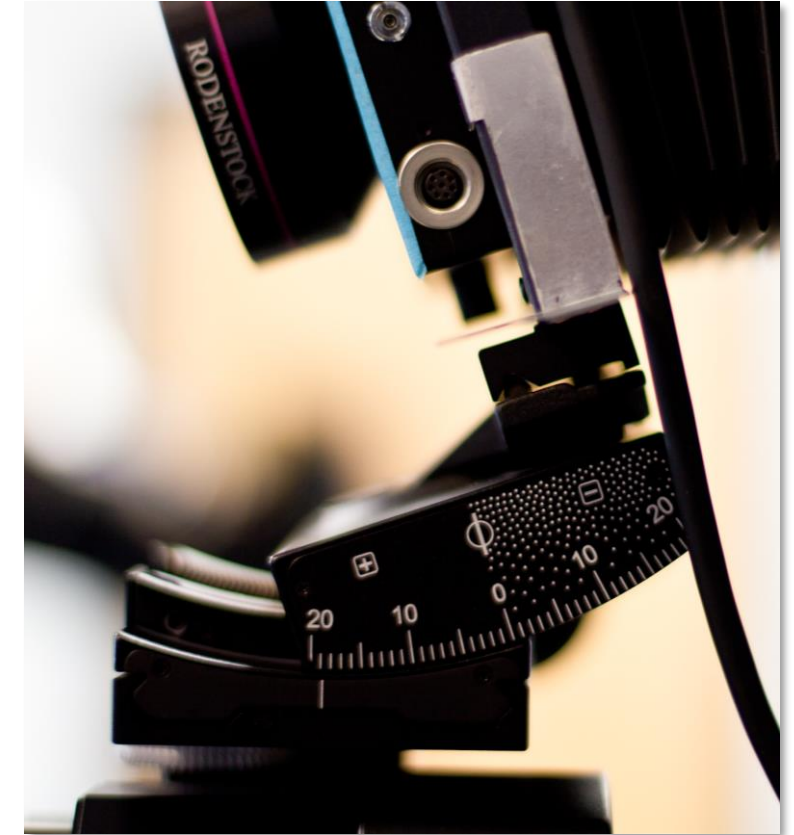
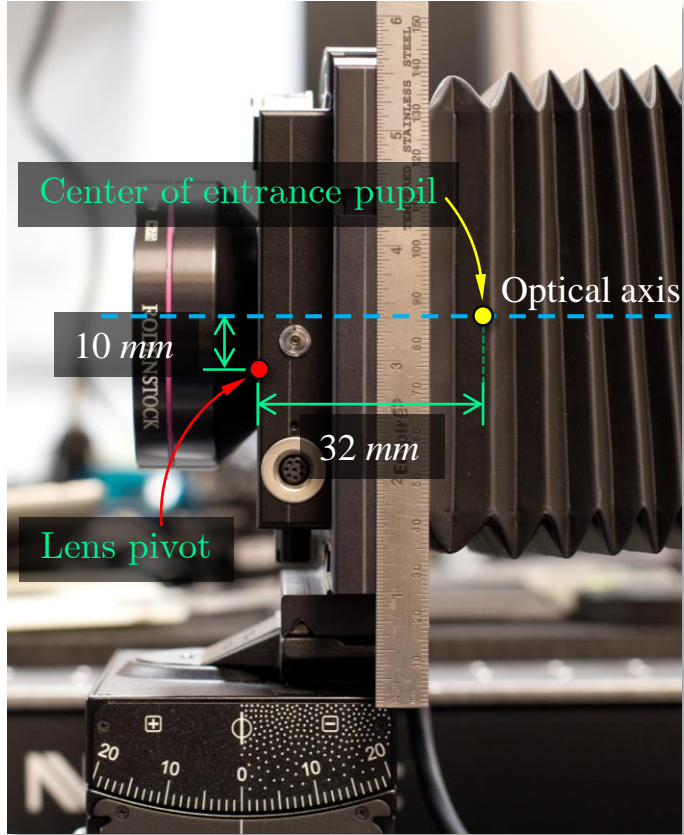
Initial experiments suggested the optics in the camera was great



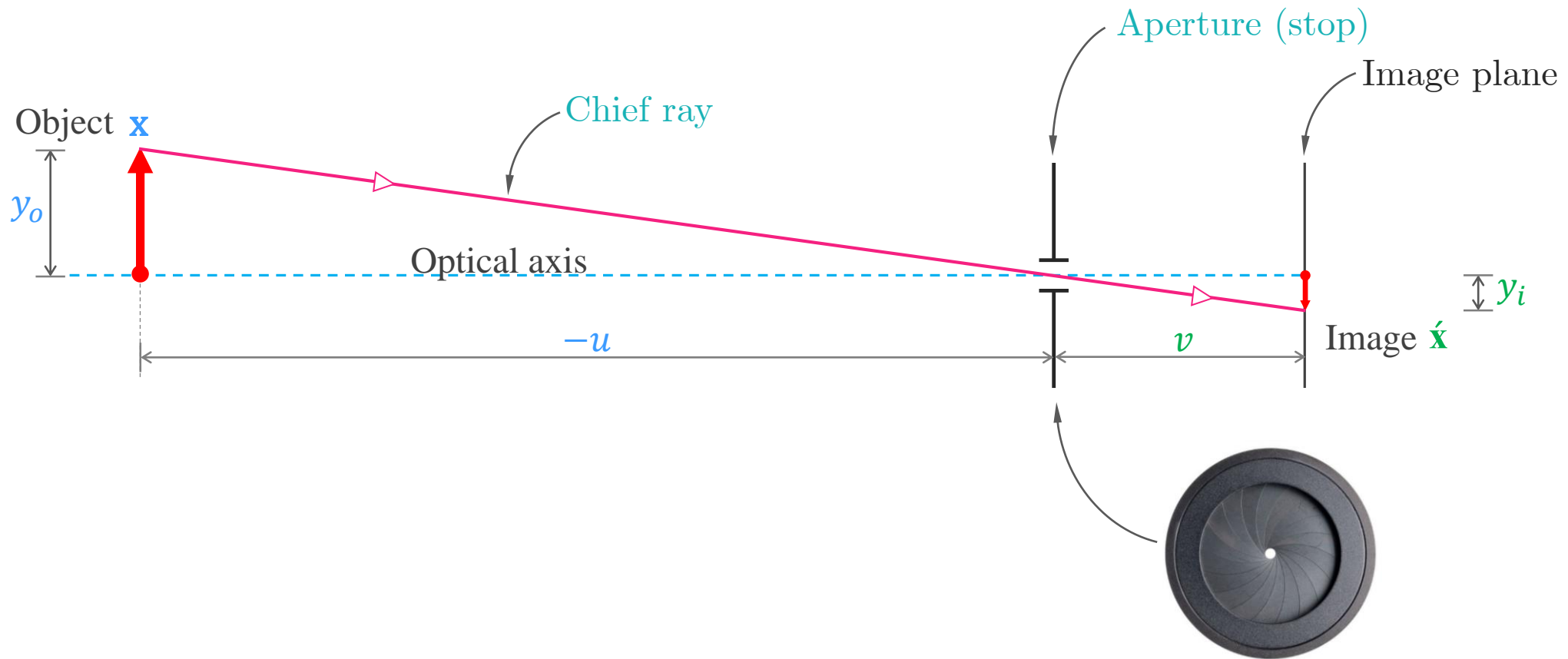
Different experimental setups in the initial stages



But that's not how things are supposed to work. Isn't it?

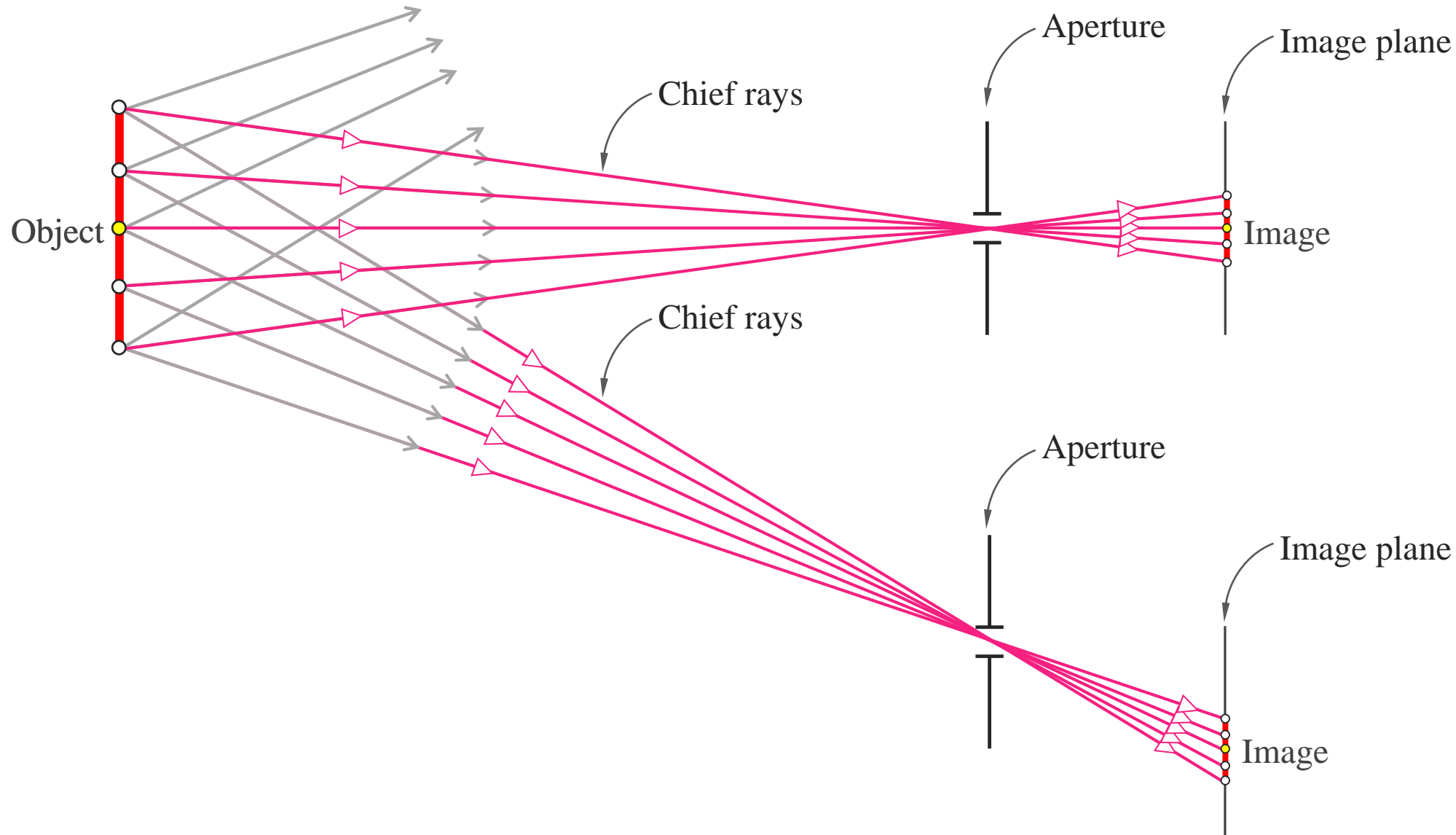


Chief rays from the object space to the image space defines the image shape

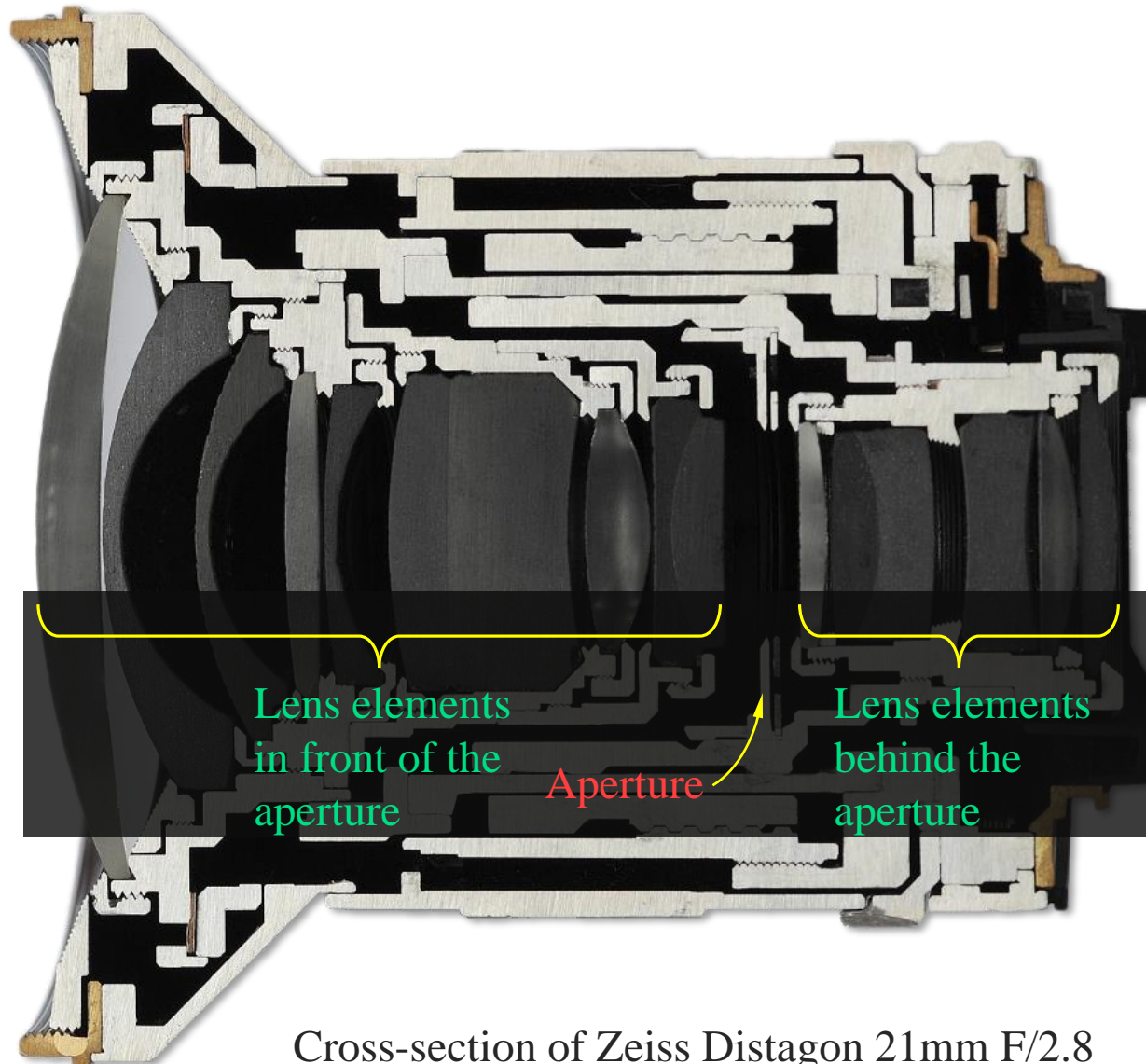


$$\text{Use of similar triangles: } m_t \text{ (transverse magnification)} = \frac{y_i}{y_o} = \frac{v}{-u} \quad \textcircled{1}$$

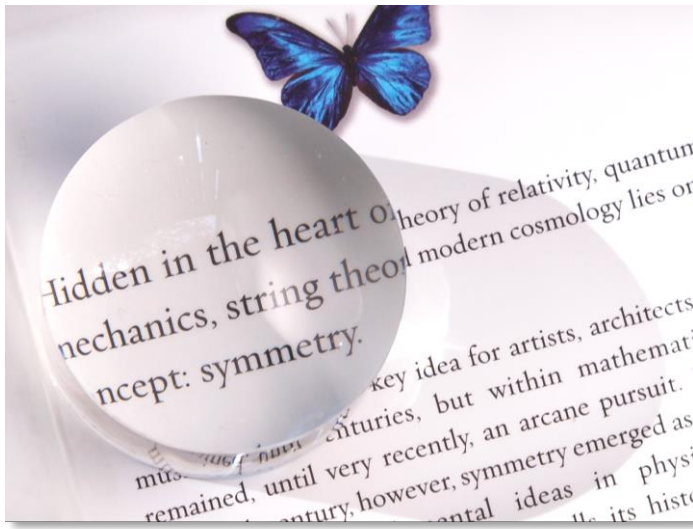
Center of perspective: the chief rays from the object space converge at the center of the aperture



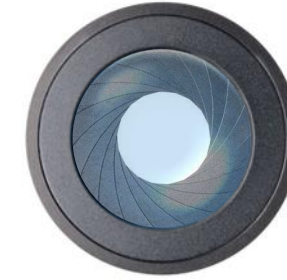
Real lenses have several refracting surfaces on either side of the aperture (stop)



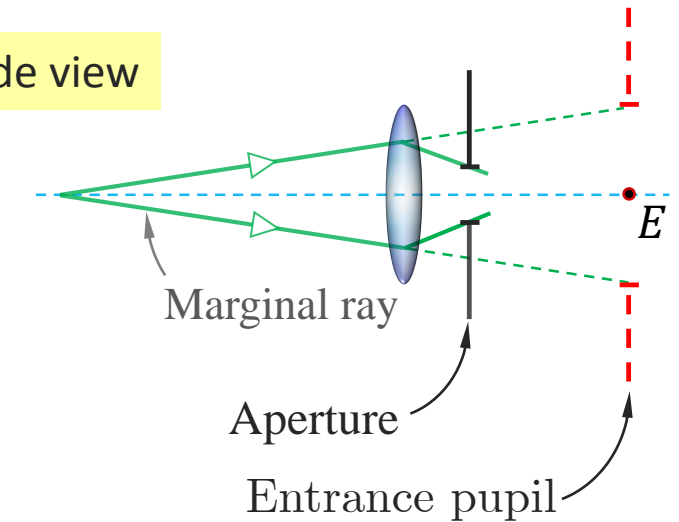
When we look into a lens we don't see the physical aperture, but rather an image of the aperture



Front view

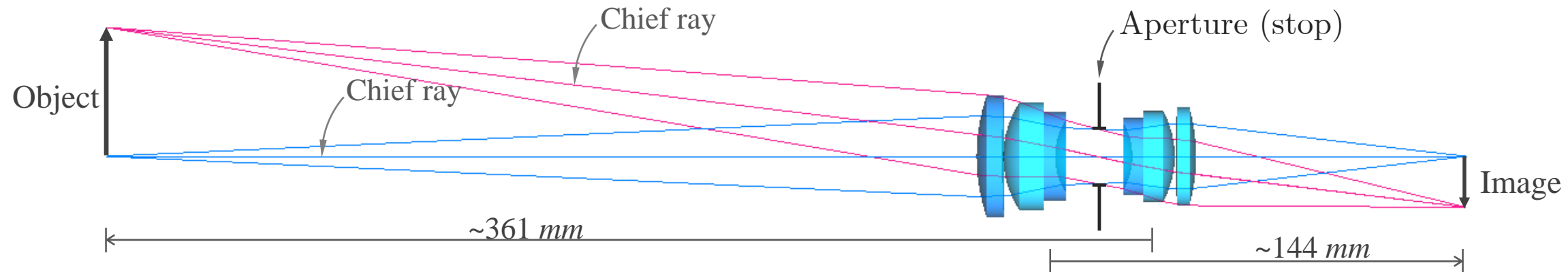


Side view

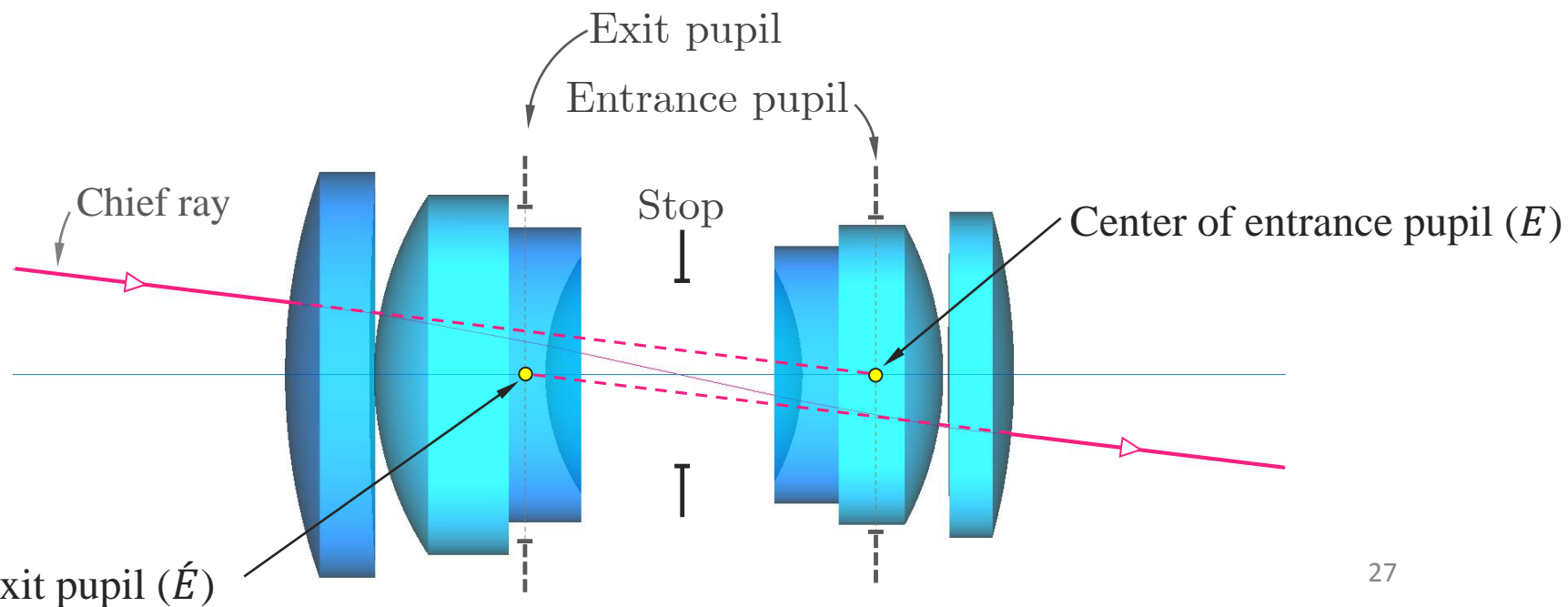


E : center of the entrance pupil

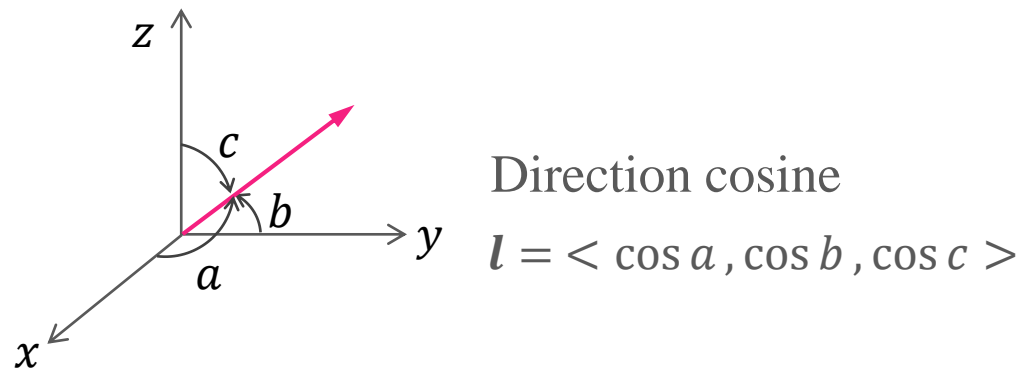
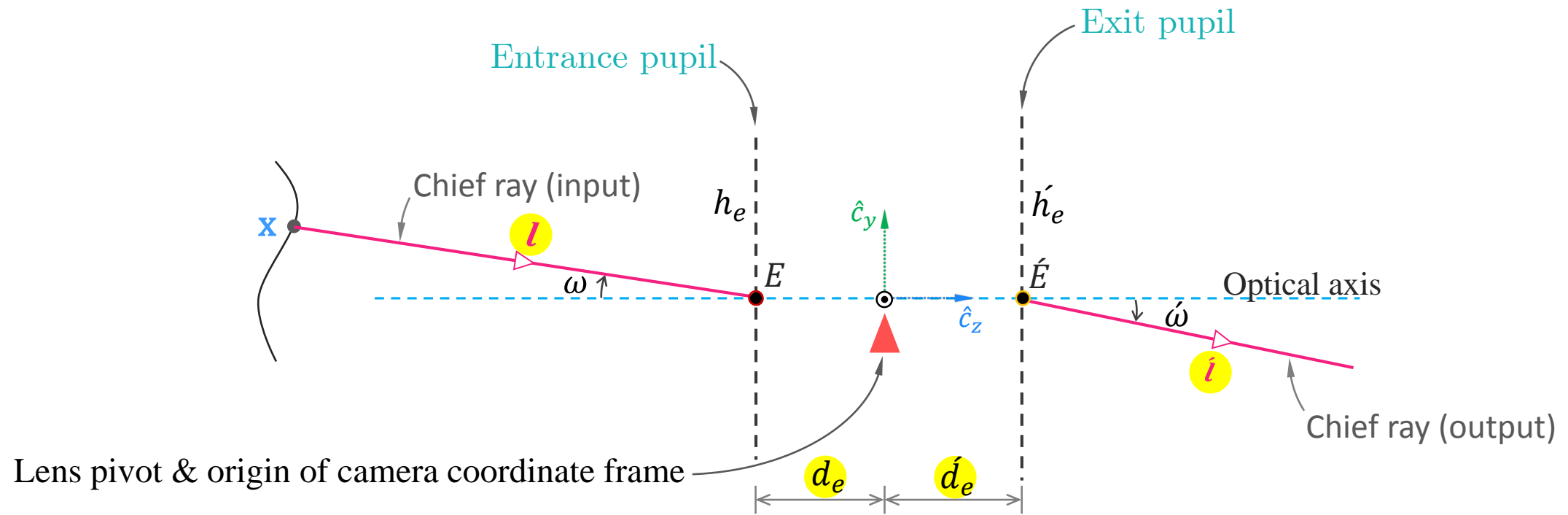
The “entrance pupil” is the image of the stop formed by the front lens elements and the “exit pupil” is the image of the stop formed by the rear lens elements



A double gauss lens ($f = 102\text{ mm}$) ▲



Nothing in optics makes sense except in the light of the pupils

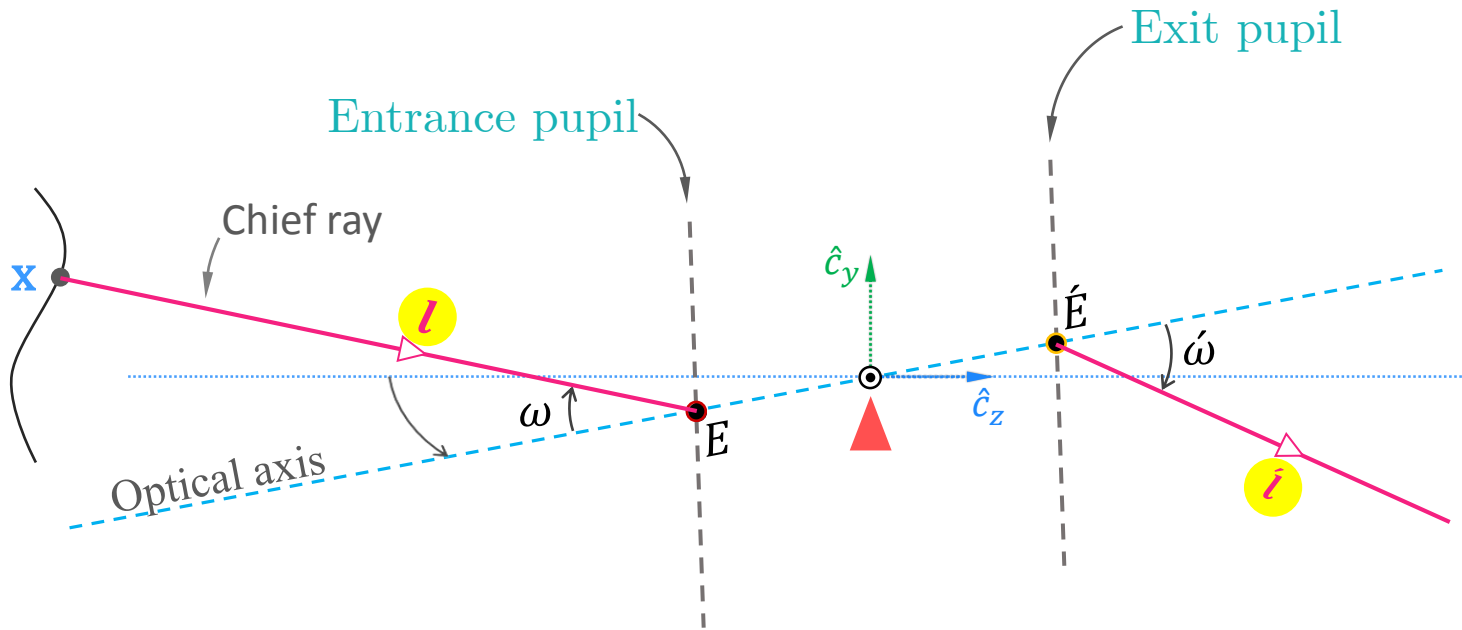


Pupil magnification:

$$m_p = \frac{\acute{h}_e}{h_e}$$

(2)

The pupil magnification m_p changes the chief ray's direction cosine in the image space



Chief ray's direction cosine
at the input (object space)

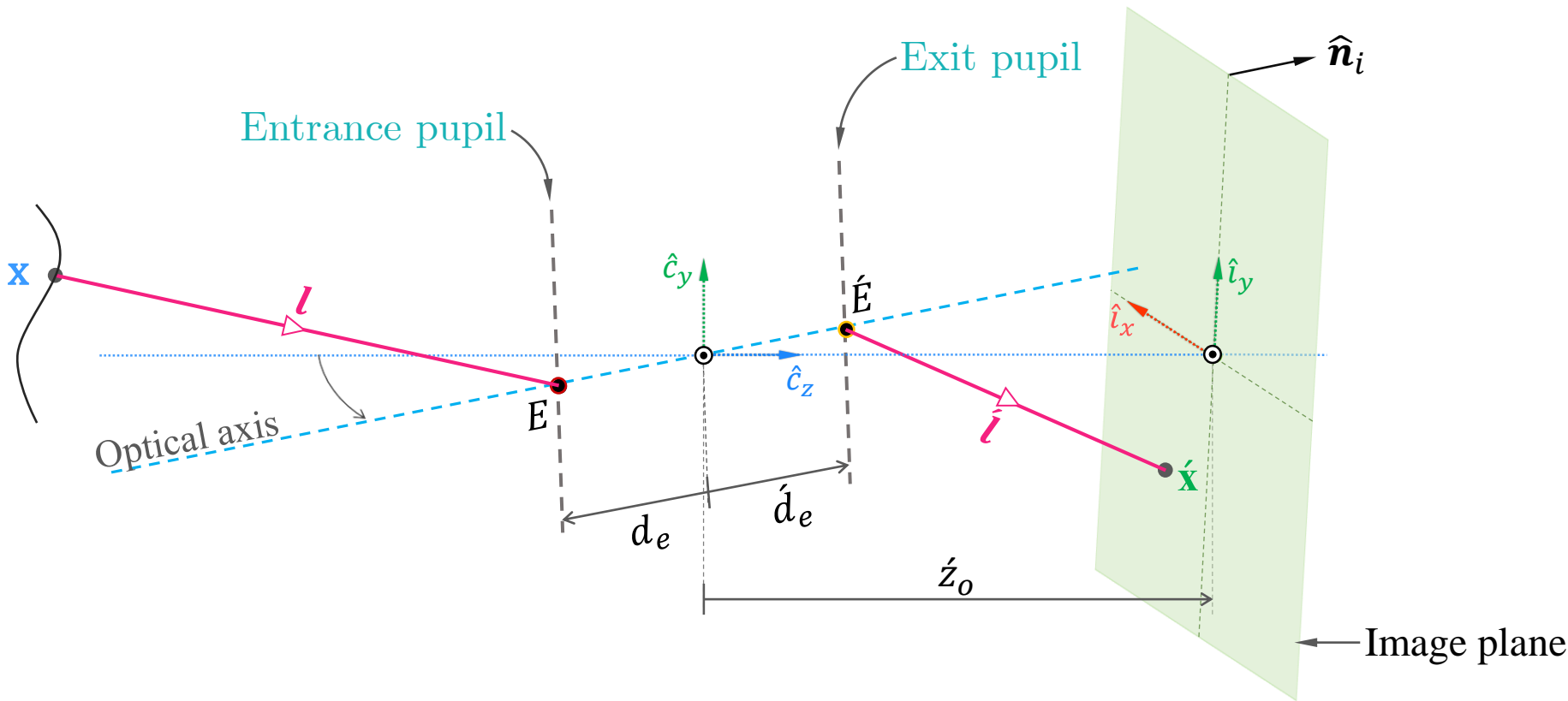
$$\hat{\mathbf{l}} = \frac{1}{\sqrt{1 + (m_p^2 - 1)n_R^2}} R_\ell M_p R_\ell^T \mathbf{l}$$

Chief ray's direction cosine at
the output (image space)

$$n_R = \mathbf{r}_{\ell,3}^T \mathbf{l}, \quad M_p = \text{diag}(1, 1, m_p)$$

③

Image-object relationship for arbitrarily oriented lens and sensor rotations



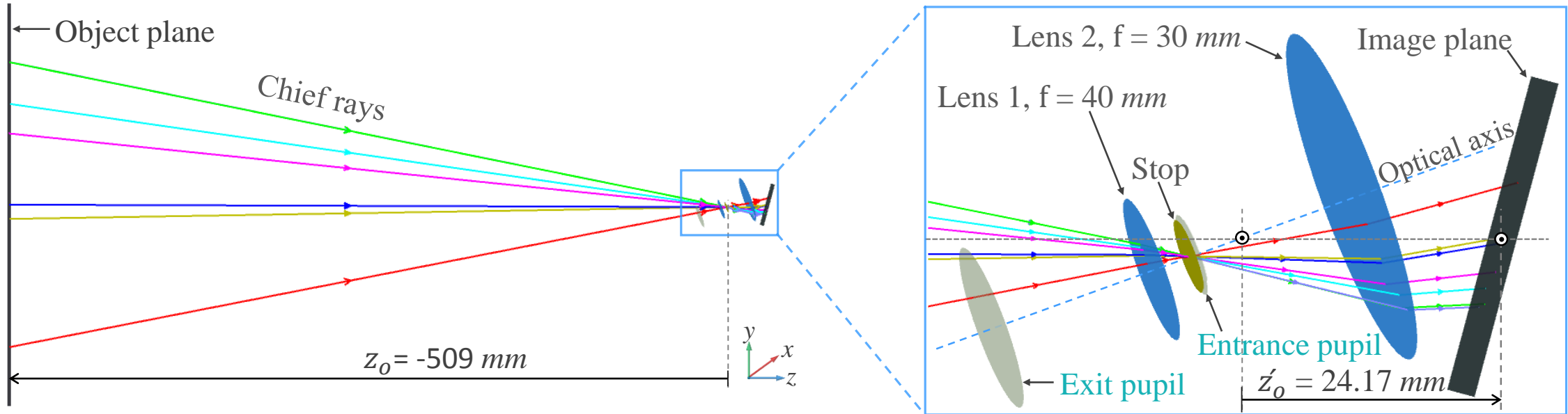
$$\acute{\mathbf{x}}' = R_i^T (\acute{\mathbf{d}}_e \mathbf{r}_{\ell,3} - \mathbf{t}_i) + \frac{(\hat{\mathbf{n}}_i(3)\acute{z}_o - \acute{\mathbf{d}}_e \hat{\mathbf{n}}_i^T \mathbf{r}_{\ell,3})}{\hat{\mathbf{n}}_i^T R_\ell \mathbf{M}_p R_\ell^T (\acute{\mathbf{c}}_x - \acute{\mathbf{d}}_e \mathbf{r}_{\ell,3})} R_i^T R_\ell \mathbf{M}_p R_\ell^T (\acute{\mathbf{c}}_x - \acute{\mathbf{d}}_e \mathbf{r}_{\ell,3})$$

Coordinates of image point
in image reference frame

Coordinates of object point
in camera frame

④

Comparing image coordinates obtained numerically against Zemax's ray traced values for randomly parameterized systems proved the accuracy of the model



Lens parameters:
 $d_e = -5 \text{ mm}$
 $\tilde{d}_e = -25 \text{ mm}$
 $f_{eff} = 24 \text{ mm}$
 $m_p = 2.0$

Lens rotation parameters:
 $\alpha_x = -20^\circ, \alpha_y = 10^\circ$

Sensor rotation parameters:
 $\beta_x = 15^\circ, \beta_y = -5^\circ$

Comparing image coordinates obtained numerically against Zemax's ray traced values for randomly parameterized systems proved the accuracy of the model

World point $c_x(x, y, z)$	Computed image point ${}^I\dot{x}(x, y, z)$	Ray-traced image point ${}^I\dot{x}_{rt}(x, y, z)$	Absolute difference $ {}^I\dot{x} - {}^I\dot{x}_{rt} $
(0.0, 0.0, -509.0)	(-0.3108, -0.6291, 0.0)	(-0.3108, -0.6291, 0.0)	(1.8e-09, 3.1e-09, 7.5e-15)
(10.0, -10.0, -509.0)	(-0.8003, -0.0863, 0.0)	(-0.8003, -0.0863, 0.0)	(2.1e-09, 2.7e-09, 3.0e-15)
(-50.0, 50.0, -509.0)	(2.1291, -3.3352, 0.0)	(2.1291, -3.3352, 0.0)	(1.2e-09, 3.2e-09, 2.9e-15)
(70.71, 70.71, -509.0)	(-4.2013, -5.0221, 0.0)	(-4.2013, -5.0221, 0.0)	(2.6e-09, 5.1e-09, 4.7e-15)
(100.0, 0.0, -509.0)	(-5.5251, -1.0101, 0.0)	(-5.5251, -1.0101, 0.0)	(1.3e-09, 8.4e-09, 3.1e-15)
(0.0, 100.0, -509.0)	(-0.6031, -6.4387, 0.0)	(-0.6031, -6.4387, 0.0)	(2.2e-09, 4.0e-09, 2.2e-16)
(100.0, 100.0, -509.0)	(-5.8238, -6.8542, 0.0)	(-5.8238, -6.8542, 0.0)	(5.6e-10, 2.5e-10, 2.2e-15)

Image distortion due to lens rotation depends on: (a) the distance of the point of rotation from the entrance pupil center, and (b) the pupil magnification m_p

Setup

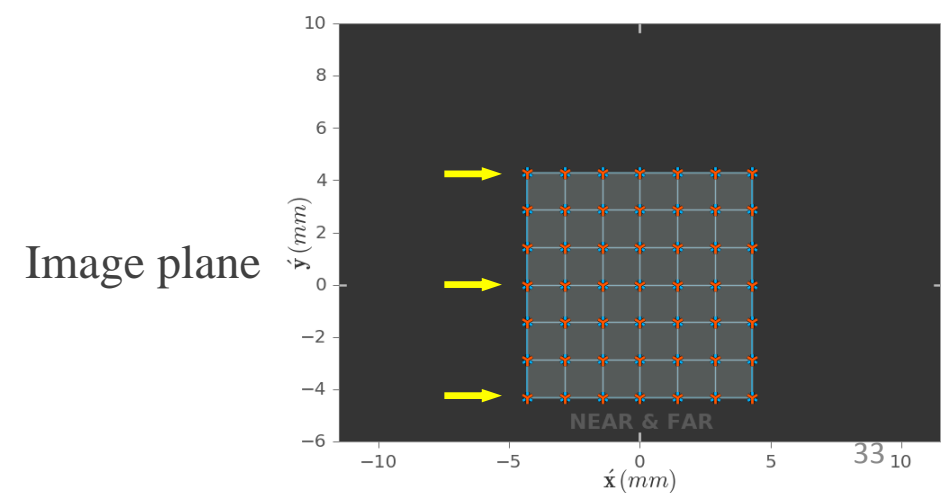
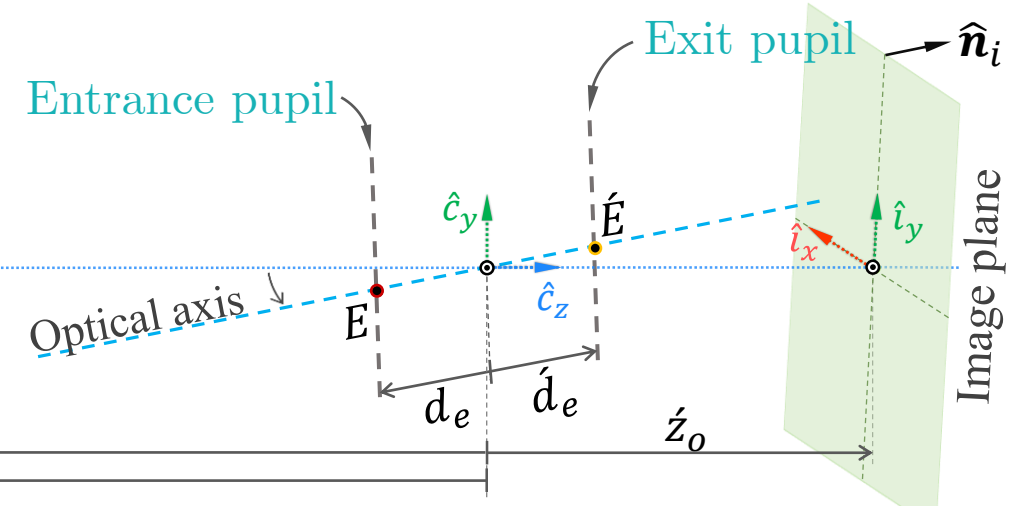
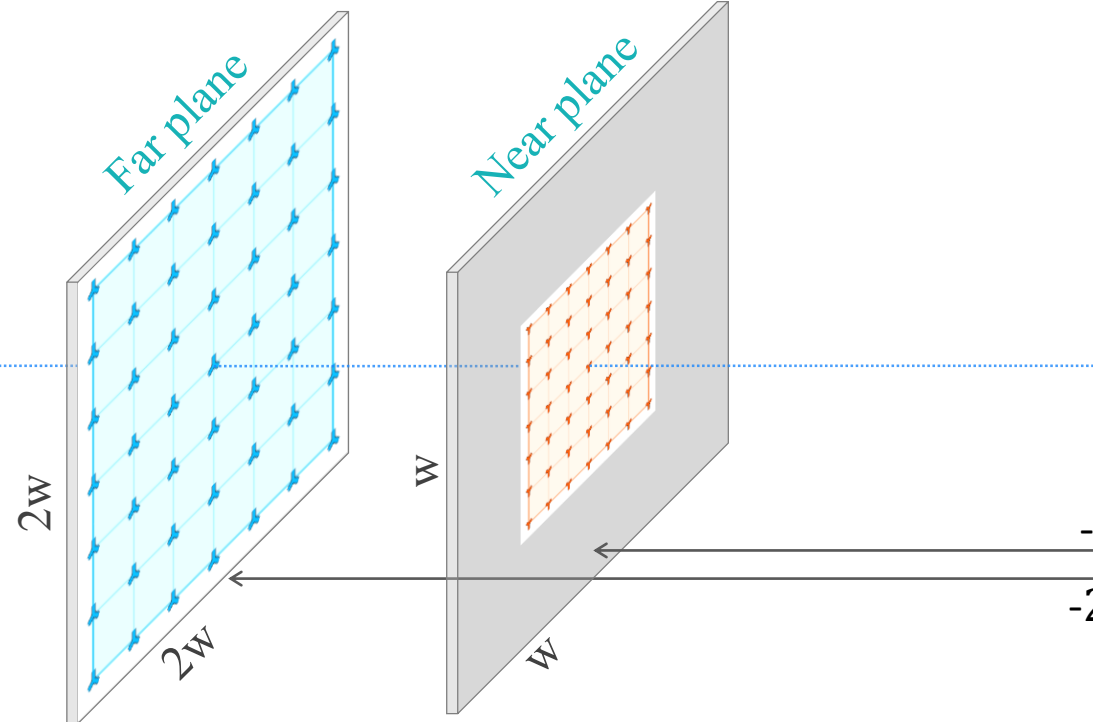
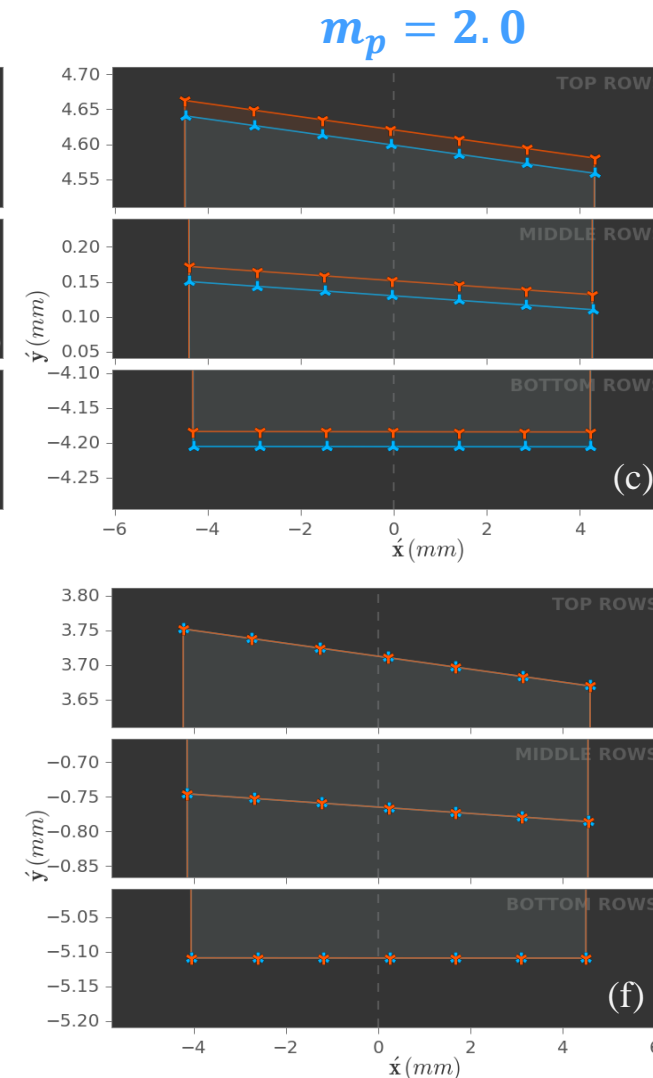
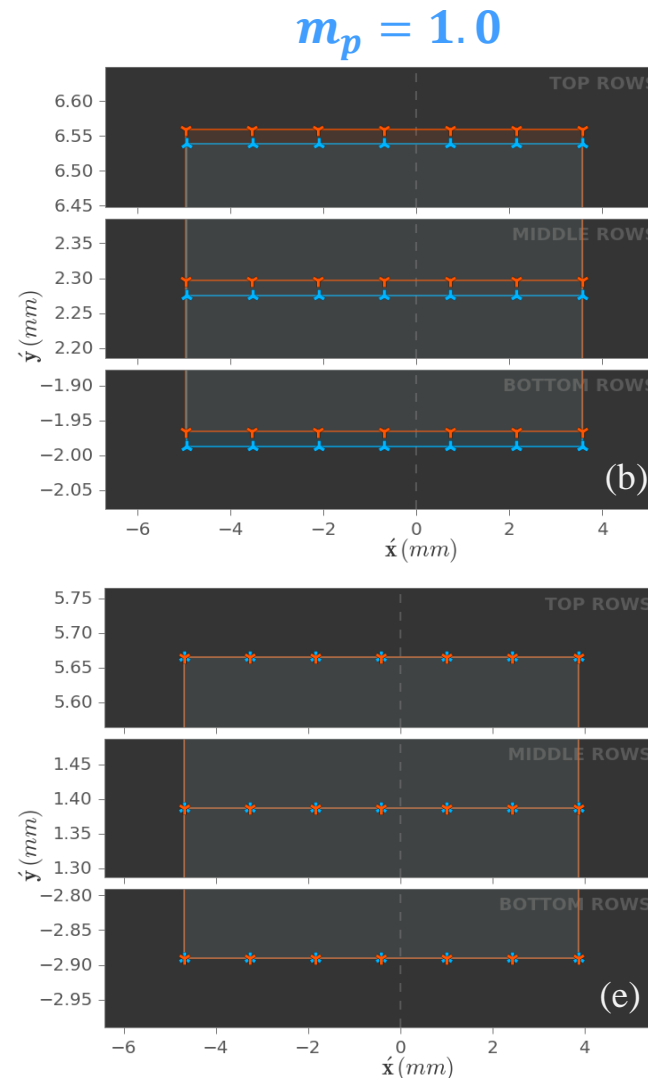
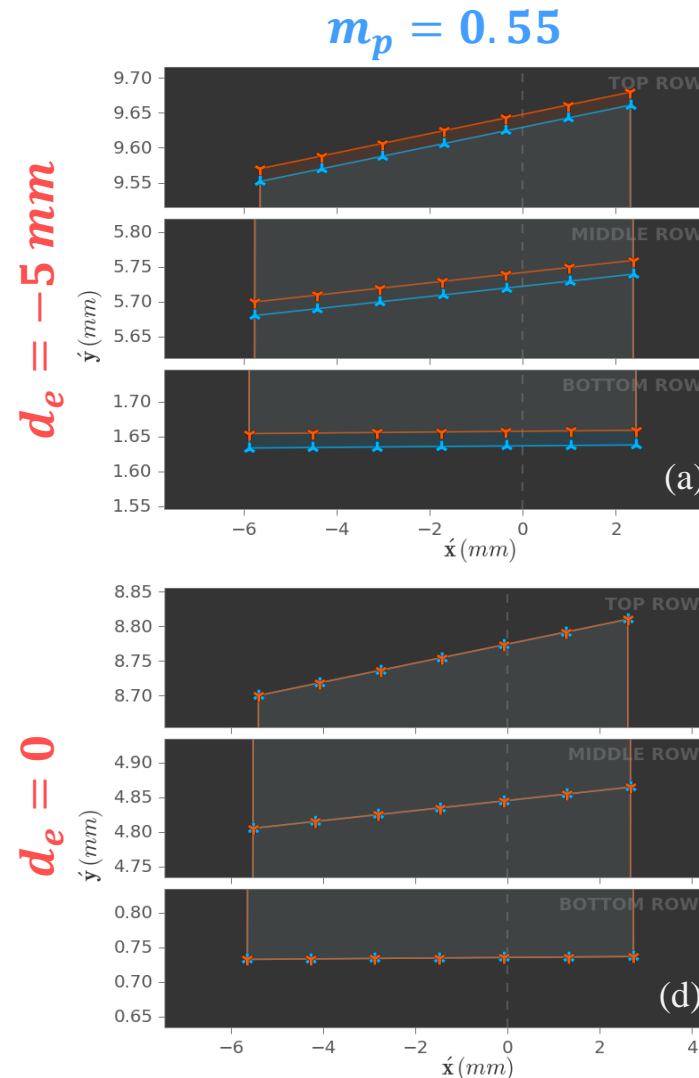
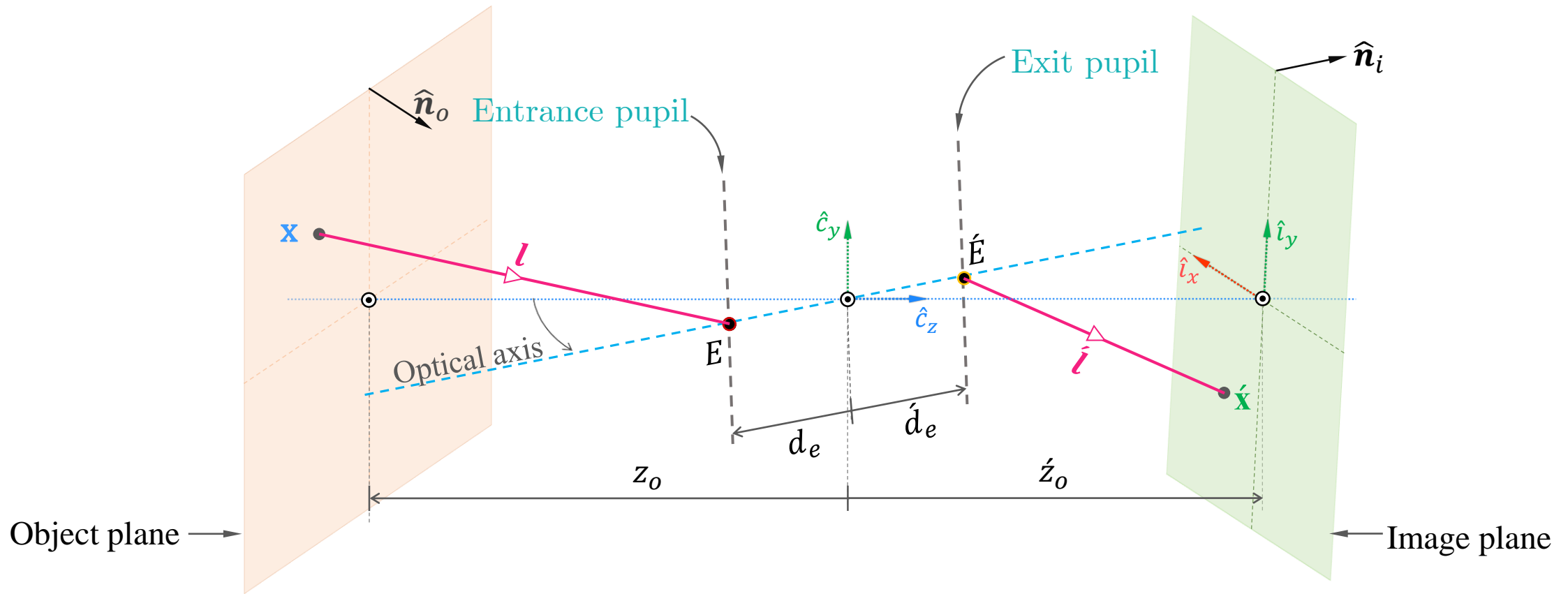


Image distortion due to lens rotation depends on: (a) the distance of the point of rotation from the entrance pupil center, and (b) the pupil magnification m_p



Focusing equation for arbitrarily oriented lens and image planes



Object orientation: $\hat{\mathbf{n}}_o$

Sensor orientation: $\hat{\mathbf{n}}_i$

Lens orientation: $R_\ell, \mathbf{r}_{\ell,3}$

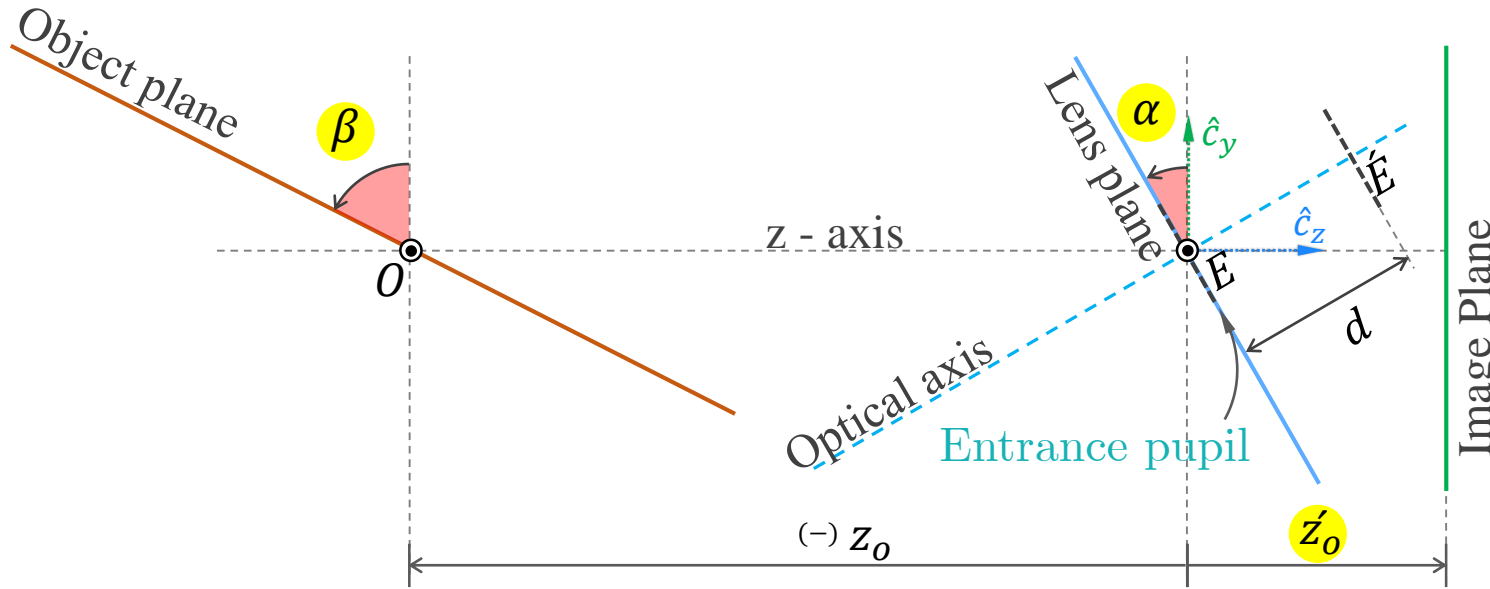
$$-\frac{\hat{\mathbf{n}}_o}{m_p[z_o - \mathbf{d}_e(\hat{\mathbf{n}}_o^T \mathbf{r}_{\ell,3})]} + \frac{R_\ell M_p R_\ell^T \hat{\mathbf{n}}_i}{[\acute{z}_o - \acute{\mathbf{d}}_e(\hat{\mathbf{n}}_i^T \mathbf{r}_{\ell,3})]} = \frac{\mathbf{r}_{\ell,3}}{f}$$

where,

$$\hat{\mathbf{n}}_o = \frac{\hat{\mathbf{n}}_o}{\hat{\mathbf{n}}_o(3)}; \quad \hat{\mathbf{n}}_i = \frac{\hat{\mathbf{n}}_i}{\hat{\mathbf{n}}_i(3)}$$

5

Focusing relations for specific configurations can be derived from the general equation: tilting a lens about its entrance pupil to focus on a tilted object plane



$$z'_o = d \cos \alpha + \frac{m_p z_o f (m_p \cos^2 \alpha + \sin^2 \alpha)}{m_p z_o \cos \alpha + f} \quad (6)$$

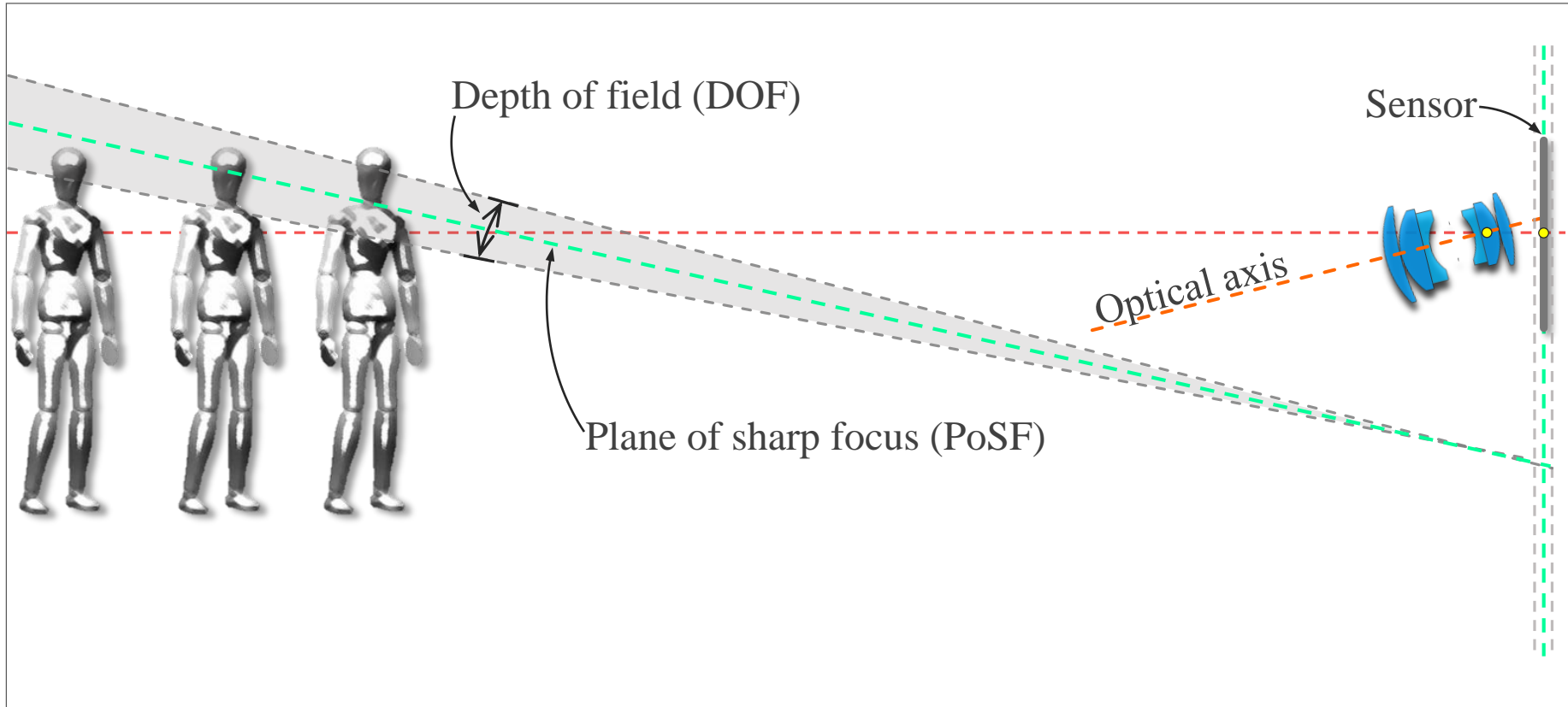
$$\tan \beta = - \frac{\sin \alpha [m_p z_o + f(1 - m_p) \cos \alpha]}{f(m_p \cos^2 \alpha + \sin^2 \alpha)} \quad (7)$$

The table demonstrates that the values of object plane tilt angle β and image plane distance z'_o in Zemax match the numerically computed values

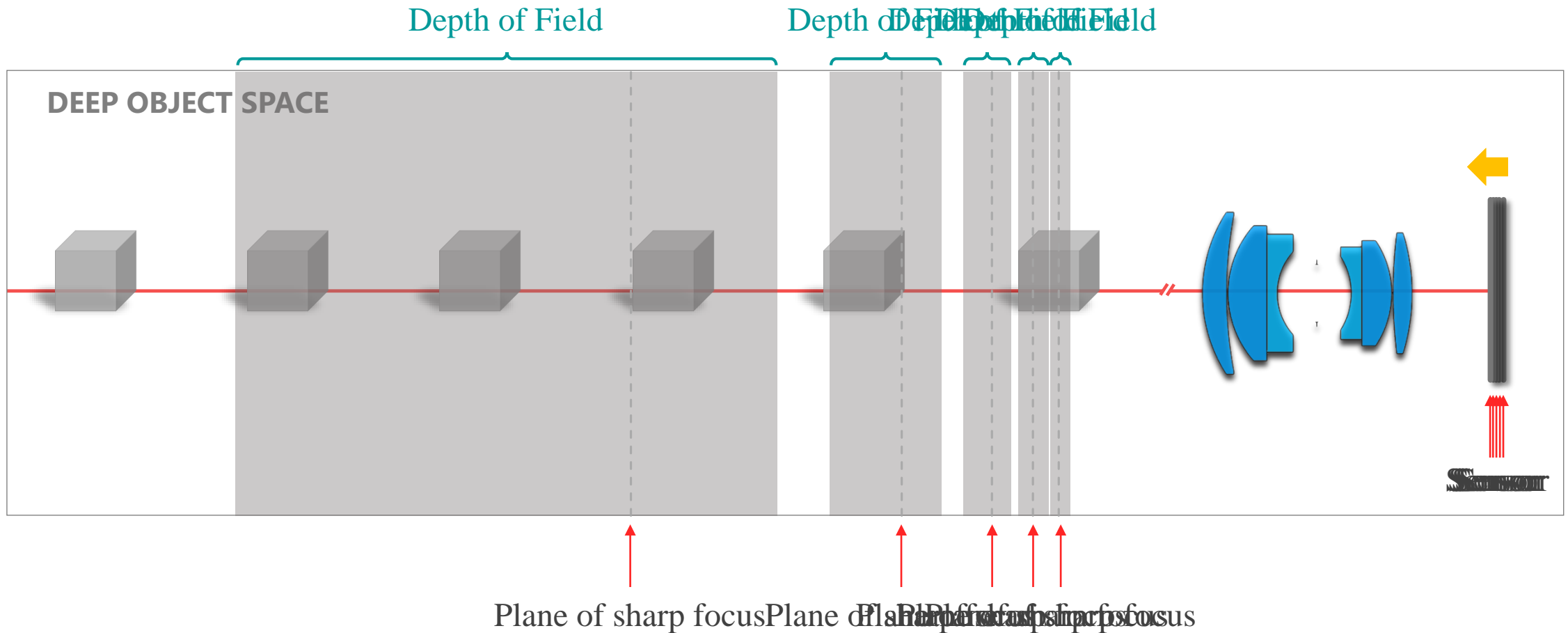
Ray traced values (Zemax)			Numerically computed	
β (Zemax) ¹	α (Zemax) ²	z'_o (Zemax) ³	β (numerical) ⁴	z'_o (numerical) ⁵
0.0°	0.0°	29.17073 mm	-2.2e-15°	29.17073 mm
-10.0°	-0.46989°	29.17145 mm	-10.0°	29.17145 mm
25.0°	1.24249°	29.17572 mm	25.0°	29.17572 mm
-40.0°	-2.23504°	29.18687 mm	-40.0°	29.18687 mm
65.0°	5.69682°	29.27607 mm	65.0°	29.27607 mm
-80.0°	-14.79587°	29.90304 mm	-80.0°	29.90304 mm

1. Object plane ($z_o = -504.0 \text{ mm}$) tilt β set in Zemax.
2. Lens plane tilt α obtained using optimization using ray-tracing in Zemax.
3. Image plane distance z'_o obtained using optimization using ray-tracing in Zemax.
4. Object plane tilt β computed numerically using the value of α in column 2.
5. Image plane distance z'_o computed numerically using the value of α in column 2.

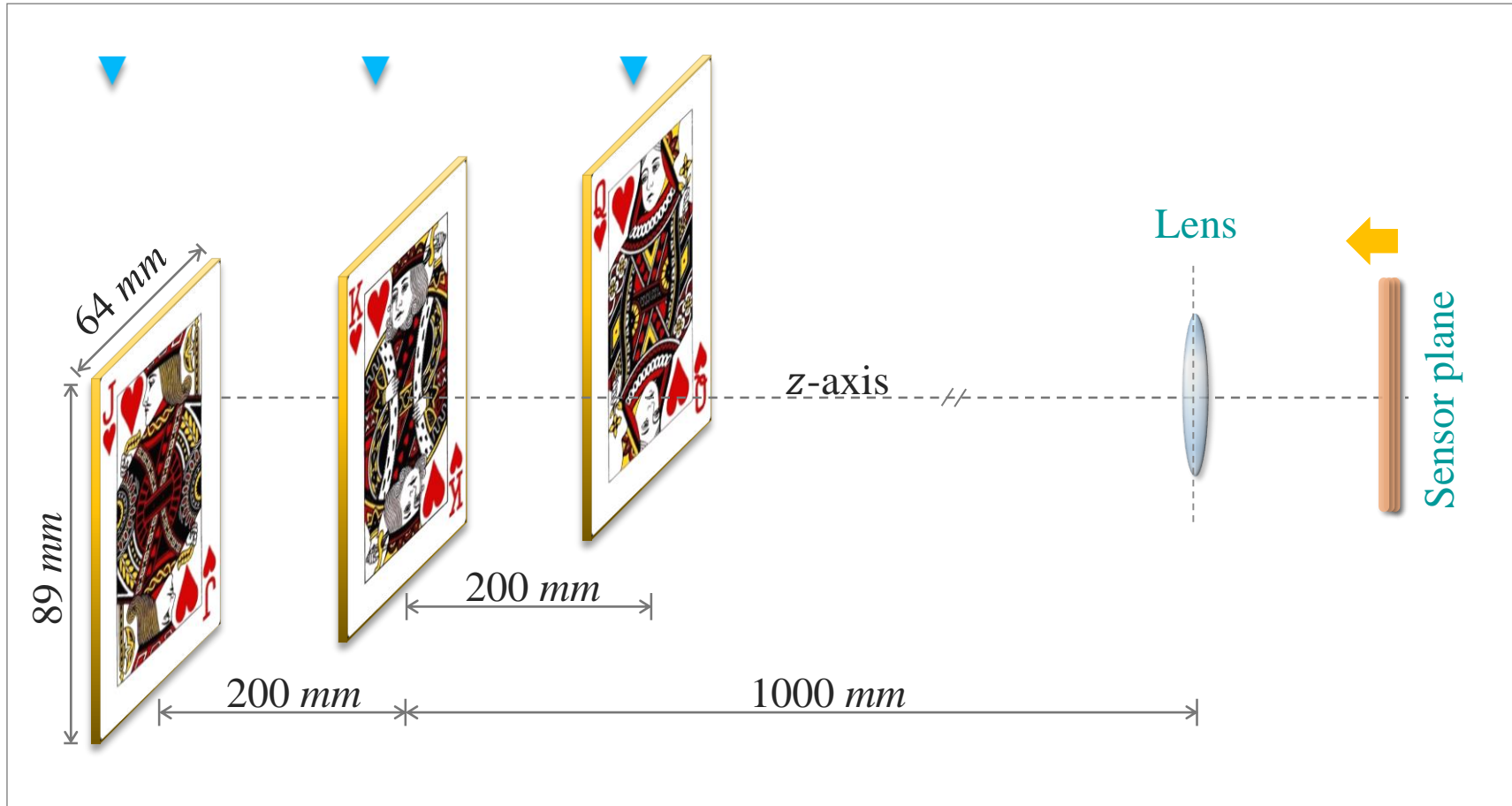
We can orient the plane of sharp focus & the DOF in Scheimpflug camera expedient to iris imaging



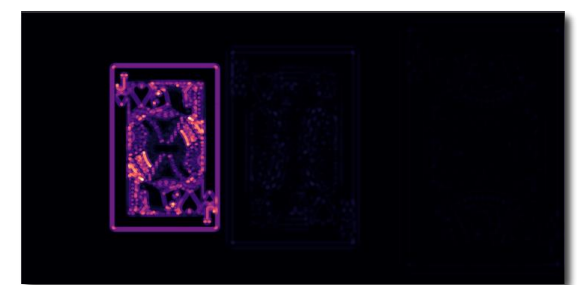
Synthesis of extended DOF in traditional photography using focus stacking



Synthesis of extended DOF in traditional photography using focus stacking



Sensor image 1/3



Focus measure (LoG)

Synthesis of extended DOF in traditional photography using focus stacking

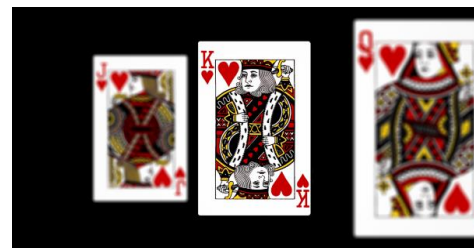
Registration



Blending



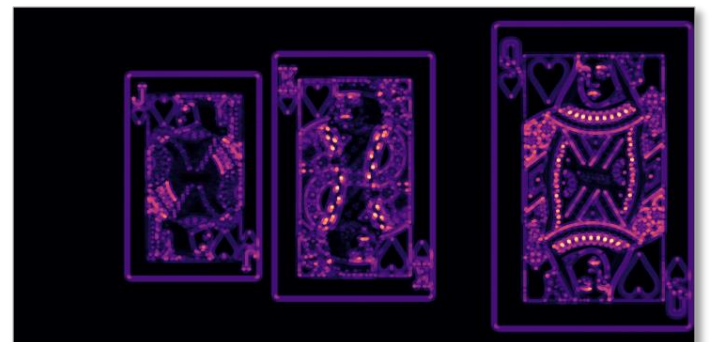
$$H_{3 \times 3}^{-1}(p)$$



$$H_{3 \times 3}^{-1}(p)$$

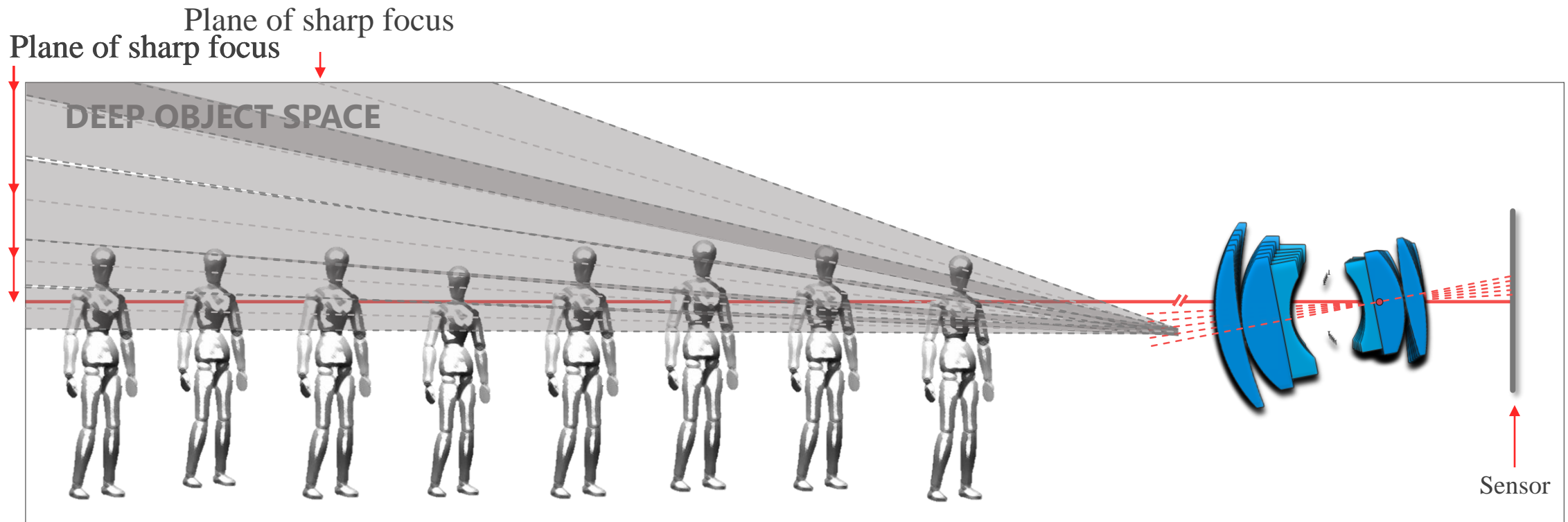


Composite image



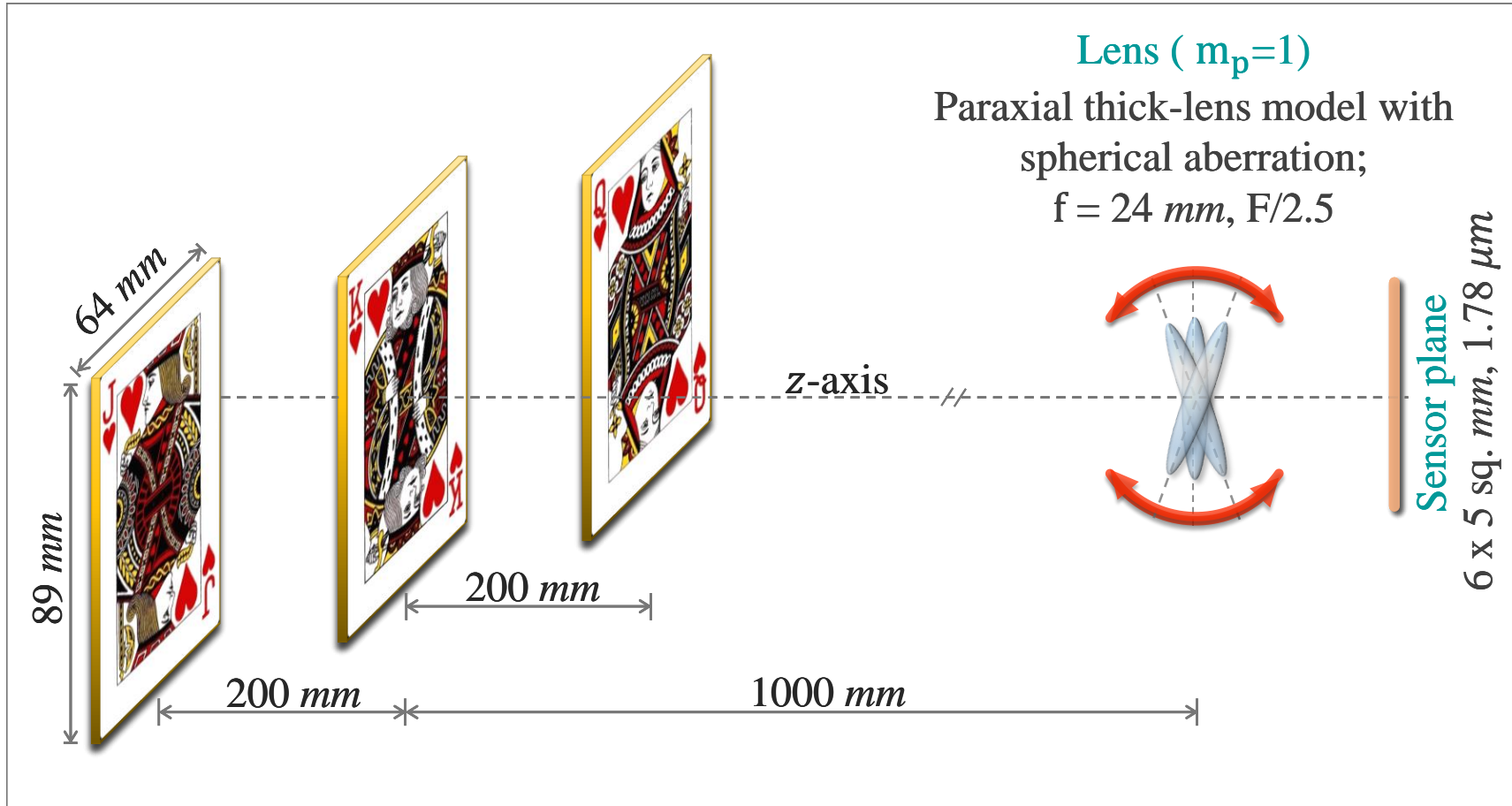
Focus measure (LoG)

So here is the idea ...

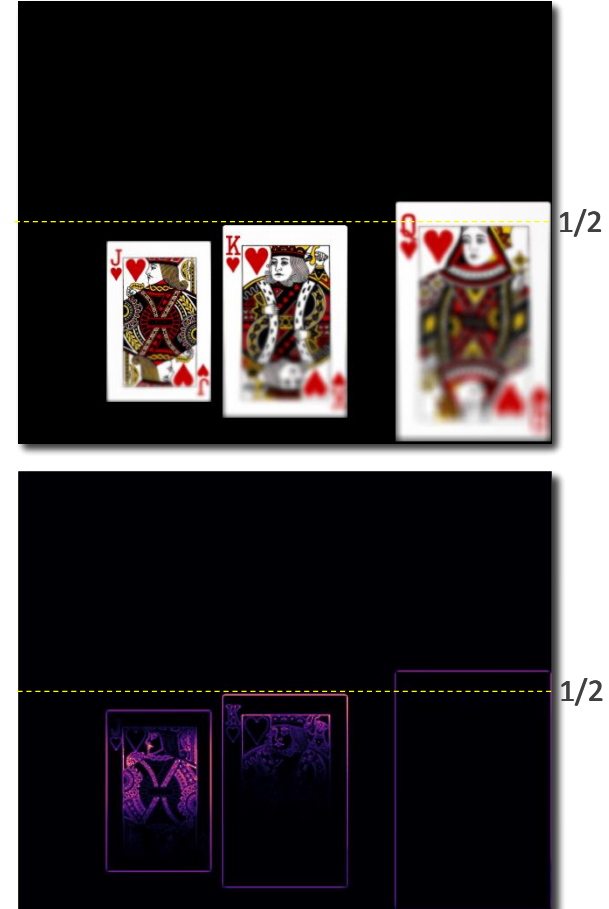


Setup of Zemax simulation to verify the theory of angular focus stacking (AFS) to extend the DOF

Lens rotated by 0.8° about ENPP

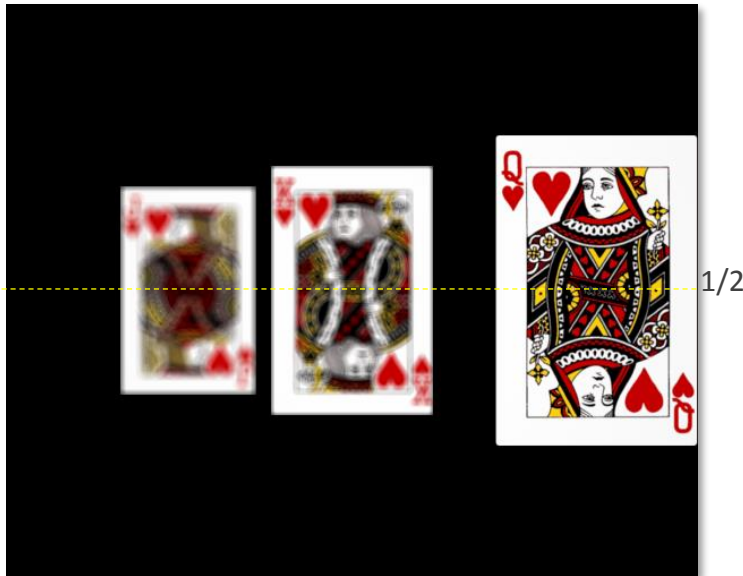


Sensor image T3/33 (0.8°)

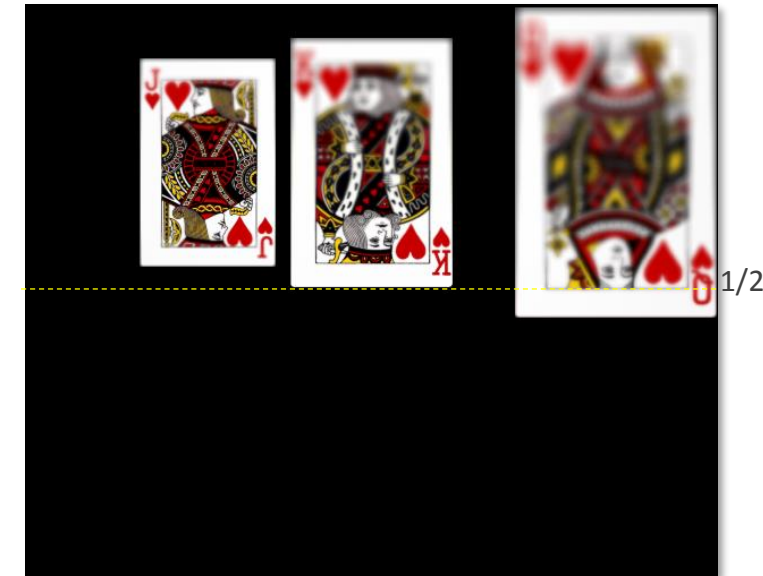


The inter-image homography is the geometric mapping between corresponding points in the images in the angular focal stack

Sensor image 1/13 (0°)



Sensor image 7/13 (-8°)



The focal stack of 13 images for lens tilts between -8° and 8°



The inter-image homography is the geometric mapping between corresponding points in the images in the angular focal stack

$${}^I\dot{\mathbf{x}} = R_i^T (\dot{d}_e \mathbf{r}_{\ell,3} - \mathbf{t}_i) + \frac{(\hat{\mathbf{n}}_i(3)\dot{z}_o - \dot{d}_e \hat{\mathbf{n}}_i^T \mathbf{r}_{\ell,3})}{\hat{\mathbf{n}}_i^T R_\ell \mathbf{M}_p R_\ell^T (\mathbf{c}_x - d_e \mathbf{r}_{\ell,3})} R_i^T R_\ell \mathbf{M}_p R_\ell^T (\mathbf{c}_x - d_e \mathbf{r}_{\ell,3}) \quad (4)$$

For rotation of a unit pupil magnification lens about the x -axis by angle α

$$\begin{bmatrix} {}^I\dot{x} \\ {}^I\dot{y} \\ 1 \end{bmatrix} = \frac{1}{c_z} \underbrace{\begin{bmatrix} (\dot{z}_o - d \cos \alpha) & 0 & 0 \\ 0 & (\dot{z}_o - d \cos \alpha) & -d \sin \alpha \\ 0 & 0 & 1 \end{bmatrix}}_{A(\alpha)} \begin{bmatrix} c_x \\ c_y \\ c_z \end{bmatrix} \quad (8)$$

Two images obtained under lens rotations α_1 and α_2 can be related as:

$${}^I\dot{\mathbf{x}}_{\alpha_2} = \underbrace{\frac{A(\alpha_2) A(\alpha_1)^{-1}}{H(\alpha_2, \alpha_1)}}_{H(\alpha_2, \alpha_1)} {}^I\dot{\mathbf{x}}_{\alpha_1} \quad (9)$$

$$H(\alpha_2, \alpha_1) = \begin{bmatrix} \frac{\dot{z}_o - d \cos \alpha_2}{\dot{z}_o - d \cos \alpha_1} & 0 & 0 \\ 0 & \frac{\dot{z}_o - d \cos \alpha_2}{\dot{z}_o - d \cos \alpha_1} & \frac{d}{p} \left(\frac{\dot{z}_o(\sin \alpha_1 - \sin \alpha_2) - d \sin(\alpha_1 - \alpha_2)}{\dot{z}_o - d \cos \alpha_1} \right) \\ 0 & 0 & 1 \end{bmatrix} \quad (10)$$

The composite image shows the complete scene in sharp focus

Registration



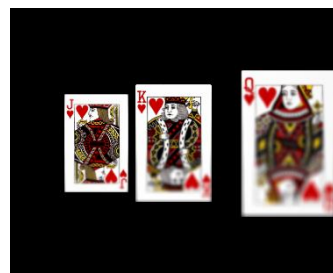
$$H_{3 \times 3}^{-1}(\alpha)$$



$$\rightarrow$$



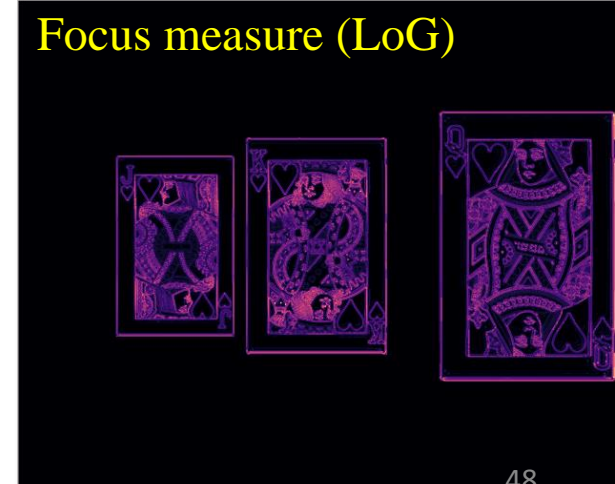
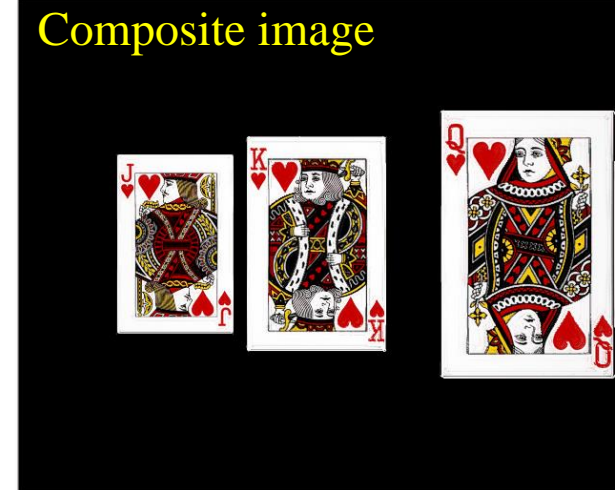
$$H_{3 \times 3}^{-1}(\alpha)$$



Blending

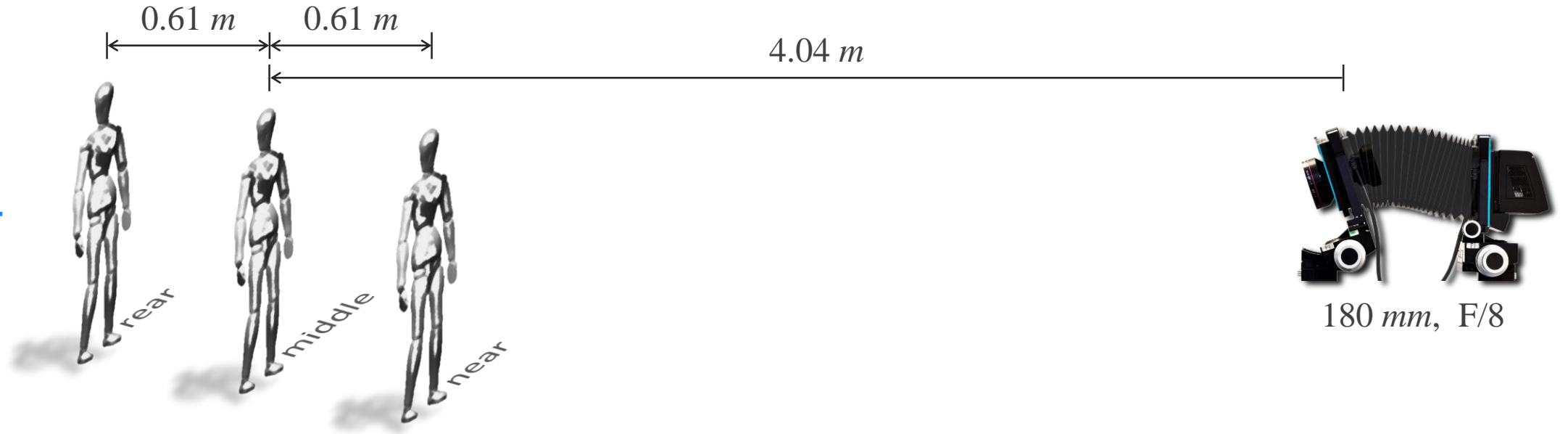


$$\rightarrow$$

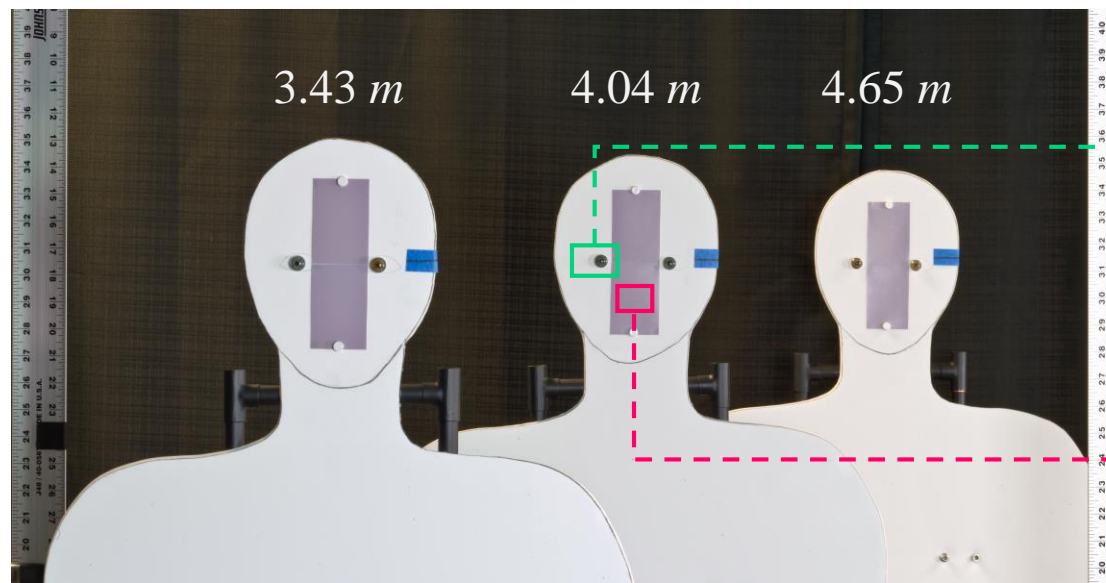


Demonstration of capture volume improvement using AFS in the laboratory

Setup #1



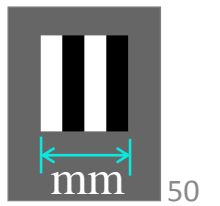
Camera's view



Artificial iris
Ø 11 mm

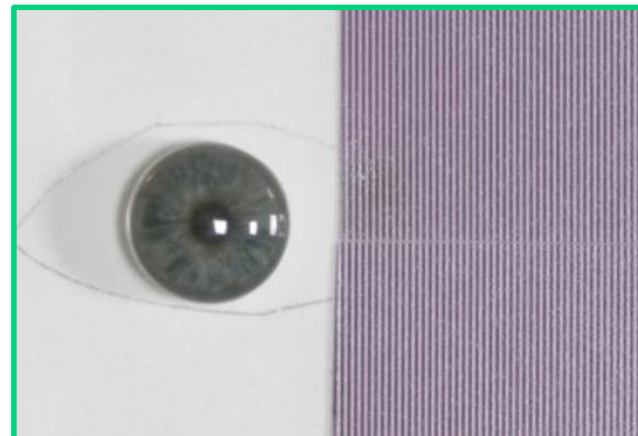
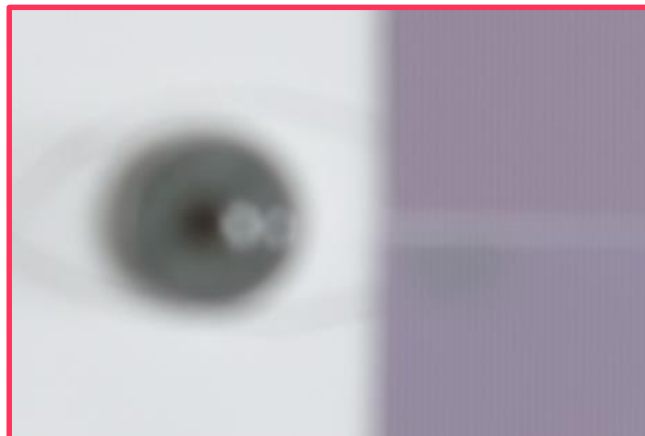
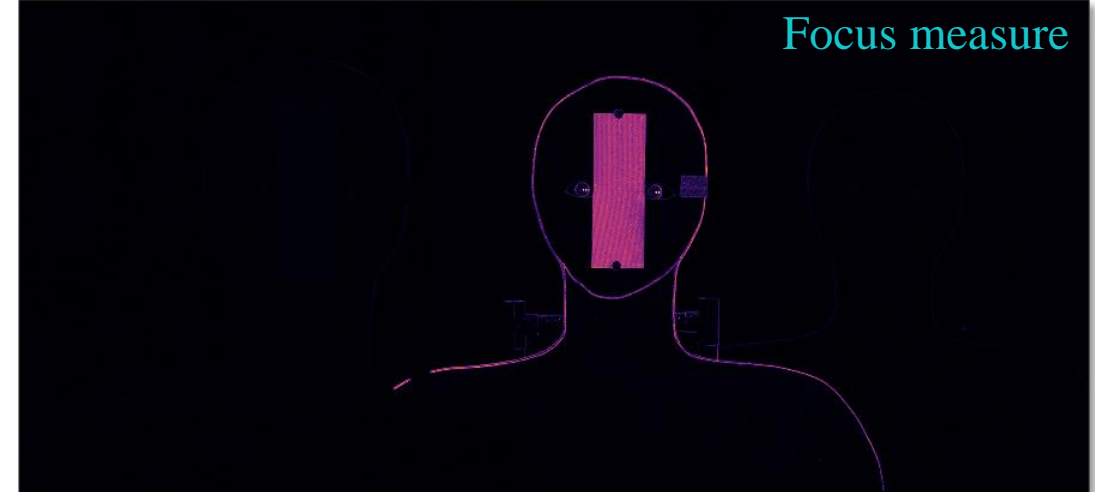
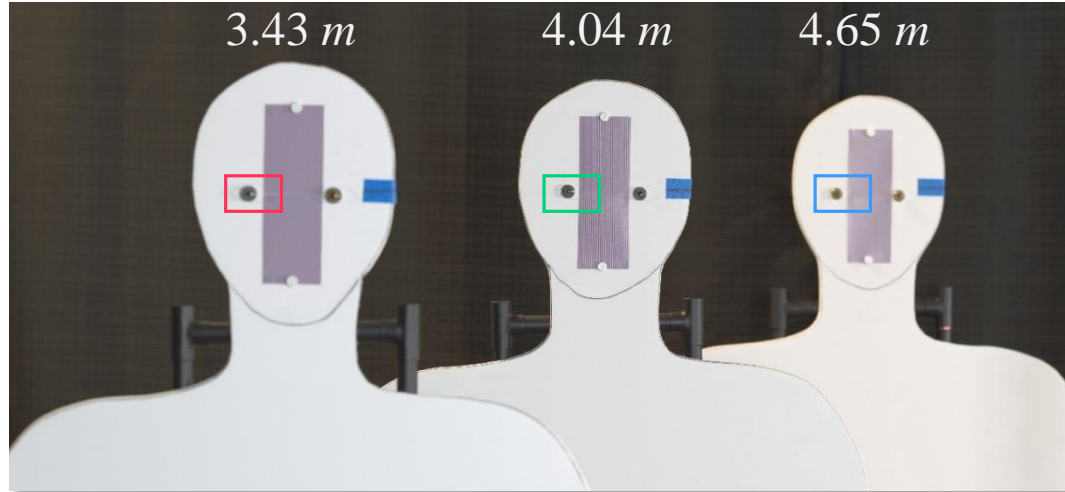


Pattern (2 lp/mm)

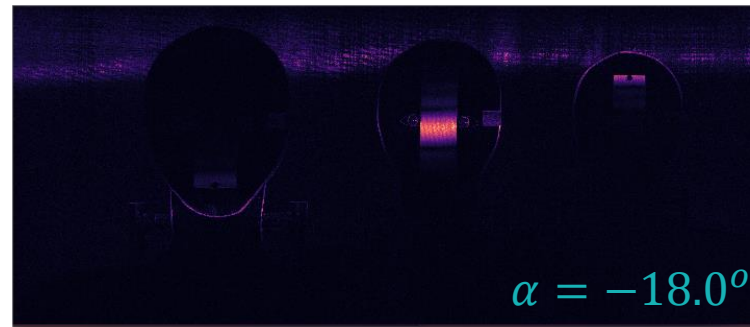
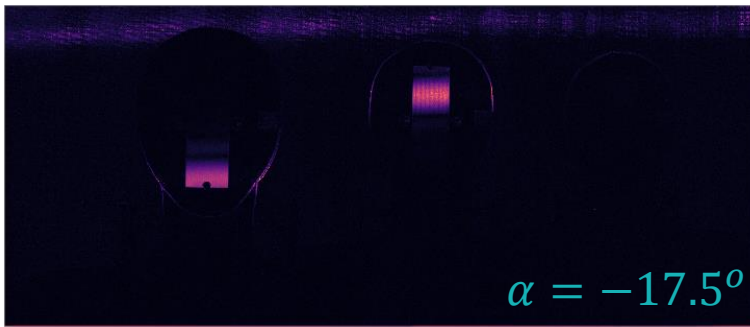


Traditional image capture with large aperture results in shallow DOF

Aperture: F/8 Exposure time: 0.77 sec Focused on: 4.04 m DOF: approx. 30 cm (for 2 lp/mm)



Focused regions in the images detected using LoG filter shows different regions of the scene in focus

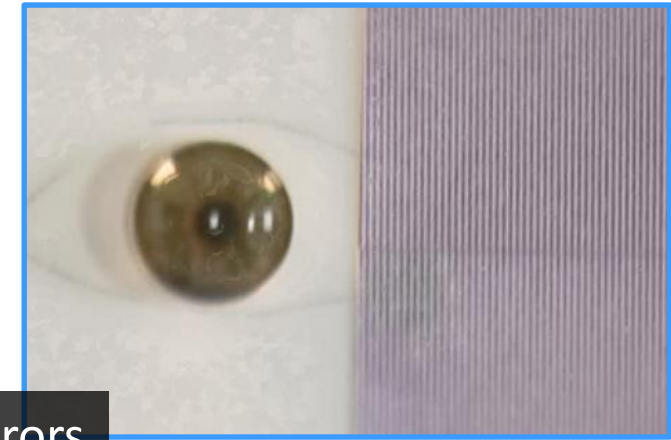
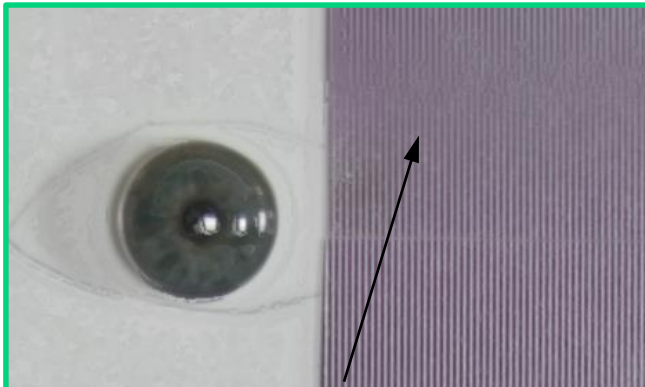
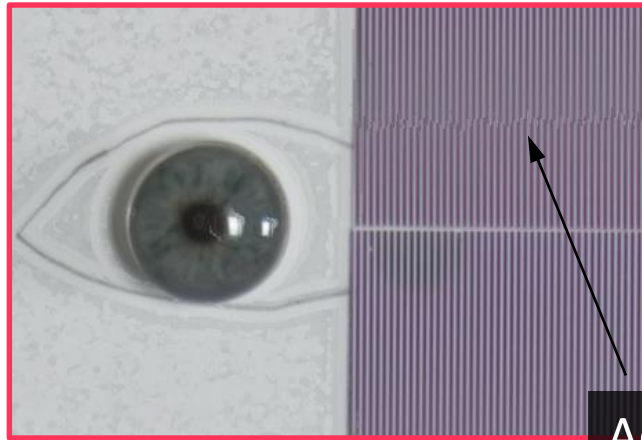
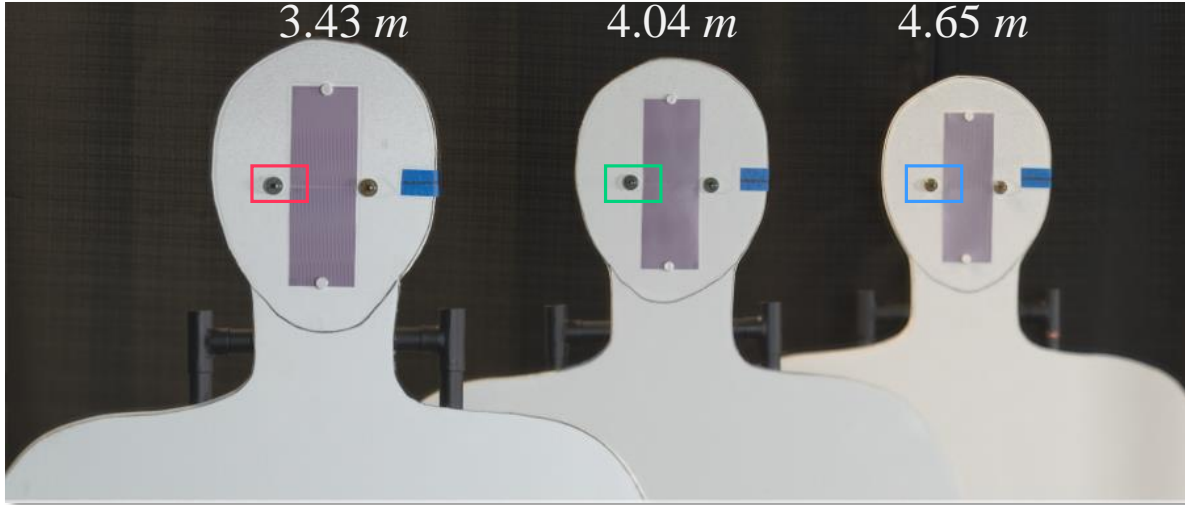


The focused regions overlaid on intensity images shows rotating the lens induces a rotation of the DOF in the object space



AFS composite image shows DOF extended beyond 1.2 meters

Aperture: F/8 (each image) Total exposure time: 5.4 sec DOF: greater than 1.2 m (for 2 lp/mm)



Adjustment errors causes registration errors

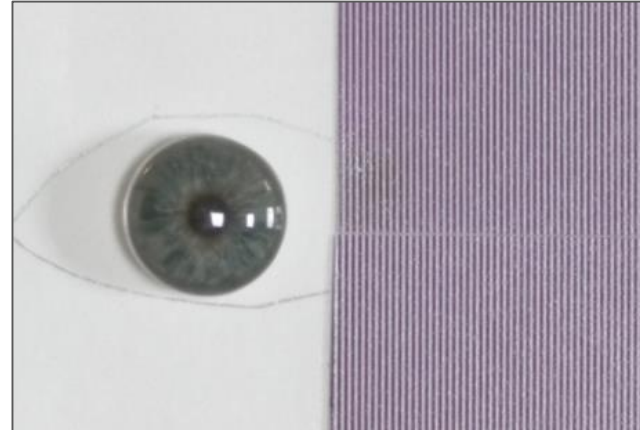
**AFS produces at least 4x more DOF than conventional imaging
for a $r_o = 2 \text{ lp/mm}$ target at 4 m**

**Conventional
at F/8**
 $\text{DOF } (r_o) = 29 \text{ cm}$

Near (3.43 m)



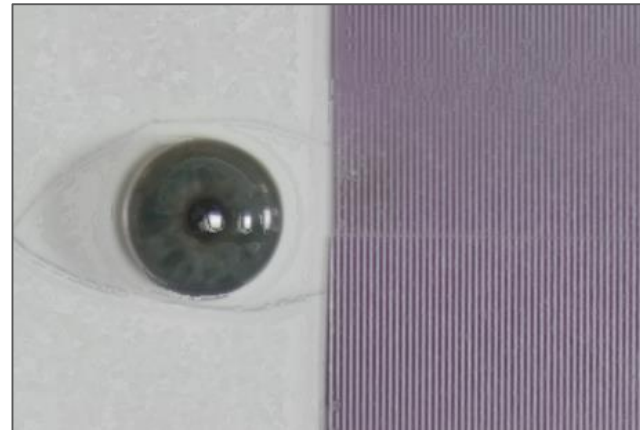
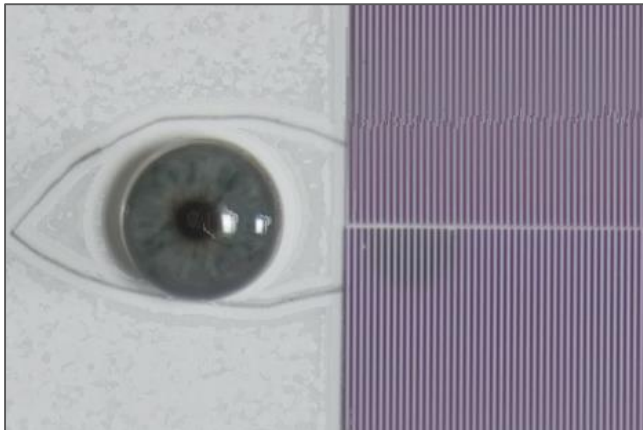
Middle (4.04 m)



Far (4.65 m)



AFS
 $\text{DOF } (r_o) \geq 1.2 \text{ m}$

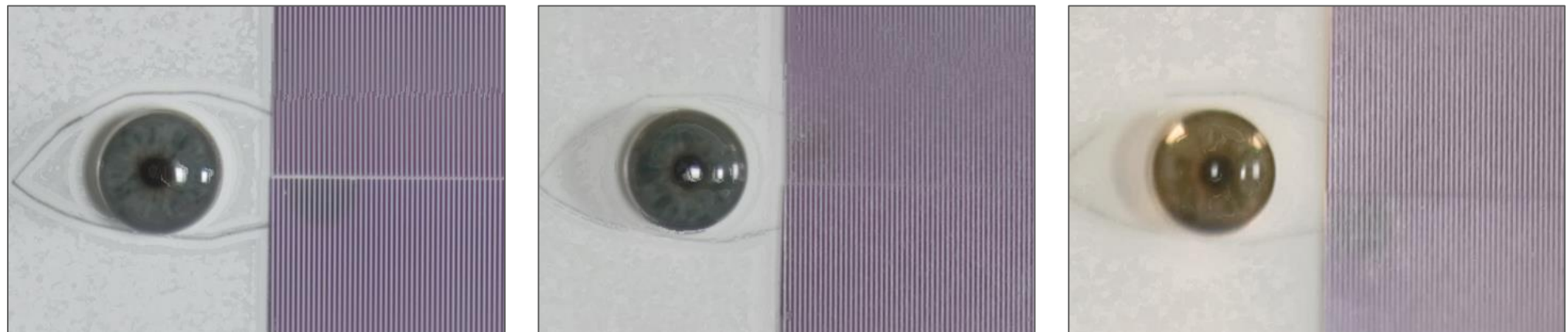


AFS is faster than conventional capture for equivalent DOF & exposure level. Therefore, subjects are less constrained within the extended capture volume.

**Conventional
at F/22
 $T = 8 \text{ sec.}$**

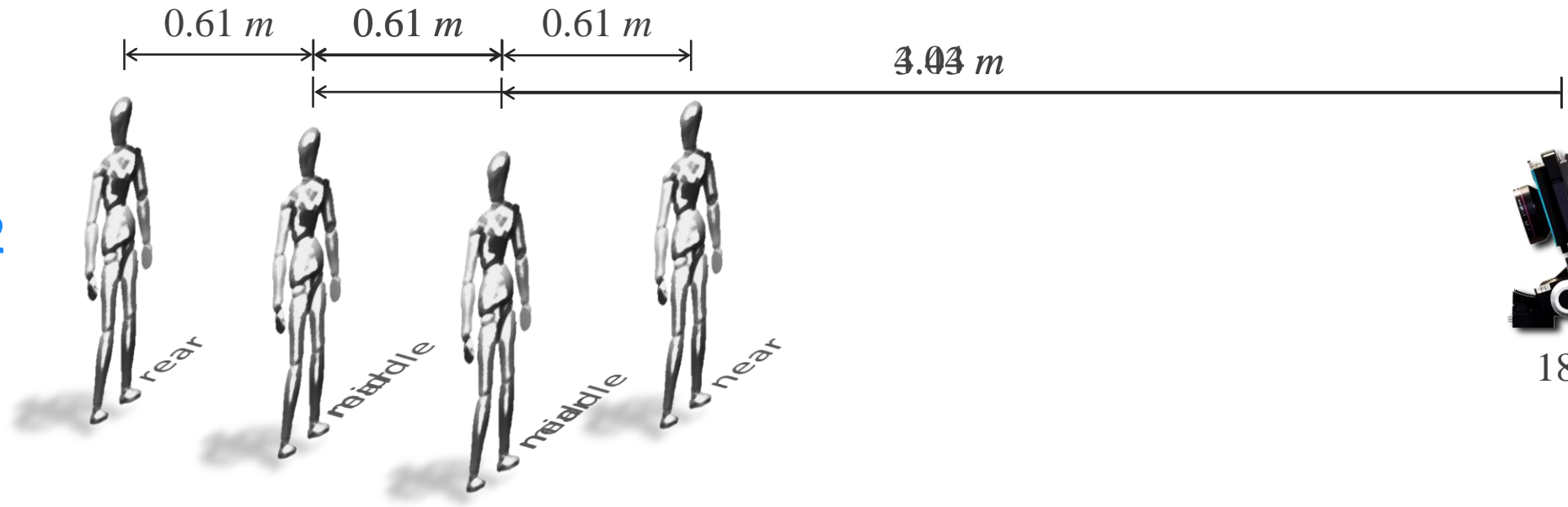


AFS
Total $T = 5 \text{ sec.}$
Each $T = 0.77 \text{ sec.}$

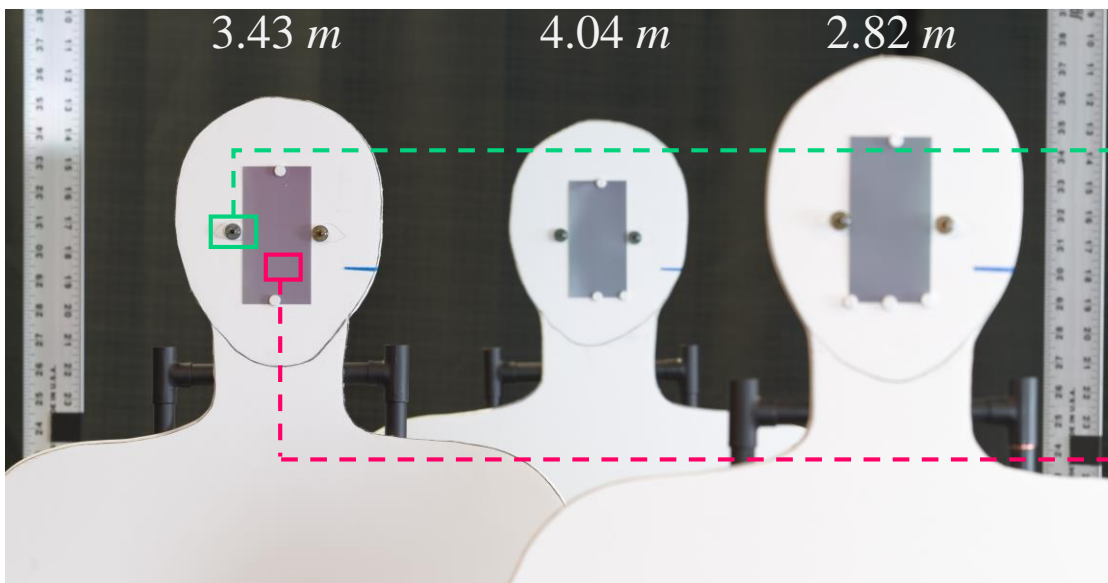


Could we push a

Setup #2



Camera's view



Artificial iris
Ø 11 mm



Pattern (3.94 lp/mm)

AFS with 14 focal stack images resulted 9.8x DOF than conventional imaging for a $r_o = 3.94 \text{ lp/mm}$ target at 3.43 m

Conventional
at F/8
DOF (r_o) = 12.5 cm



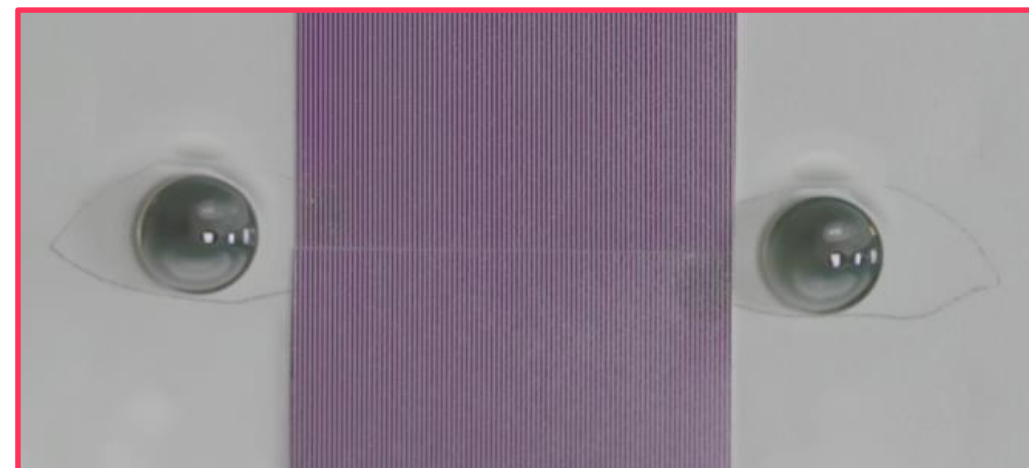
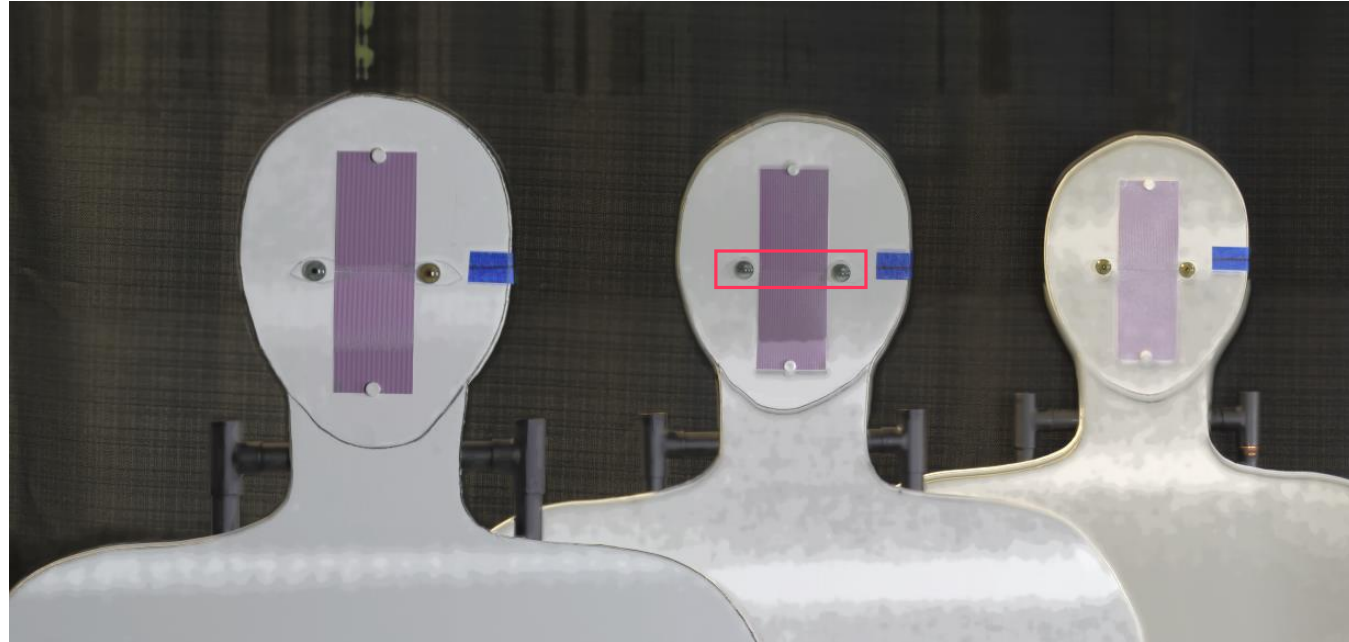
AFS*
DOF (r_o) $\geq 1.2 \text{ m}$



*In this example, the focal stack images, after registration, were fused using Helicon focus.

Automatic registration and image fusion fails if the lens is not rotated about the center of the entrance pupil

Output of Helicon
focus



Angular focus stacking method provides several advantages for extending the capture volume

- The method is simple
- Low computational complexity
- Easily scalable
- Allows the break free from traditional optical imaging tradeoffs of resolution, DOF and noise
- Faster capture time